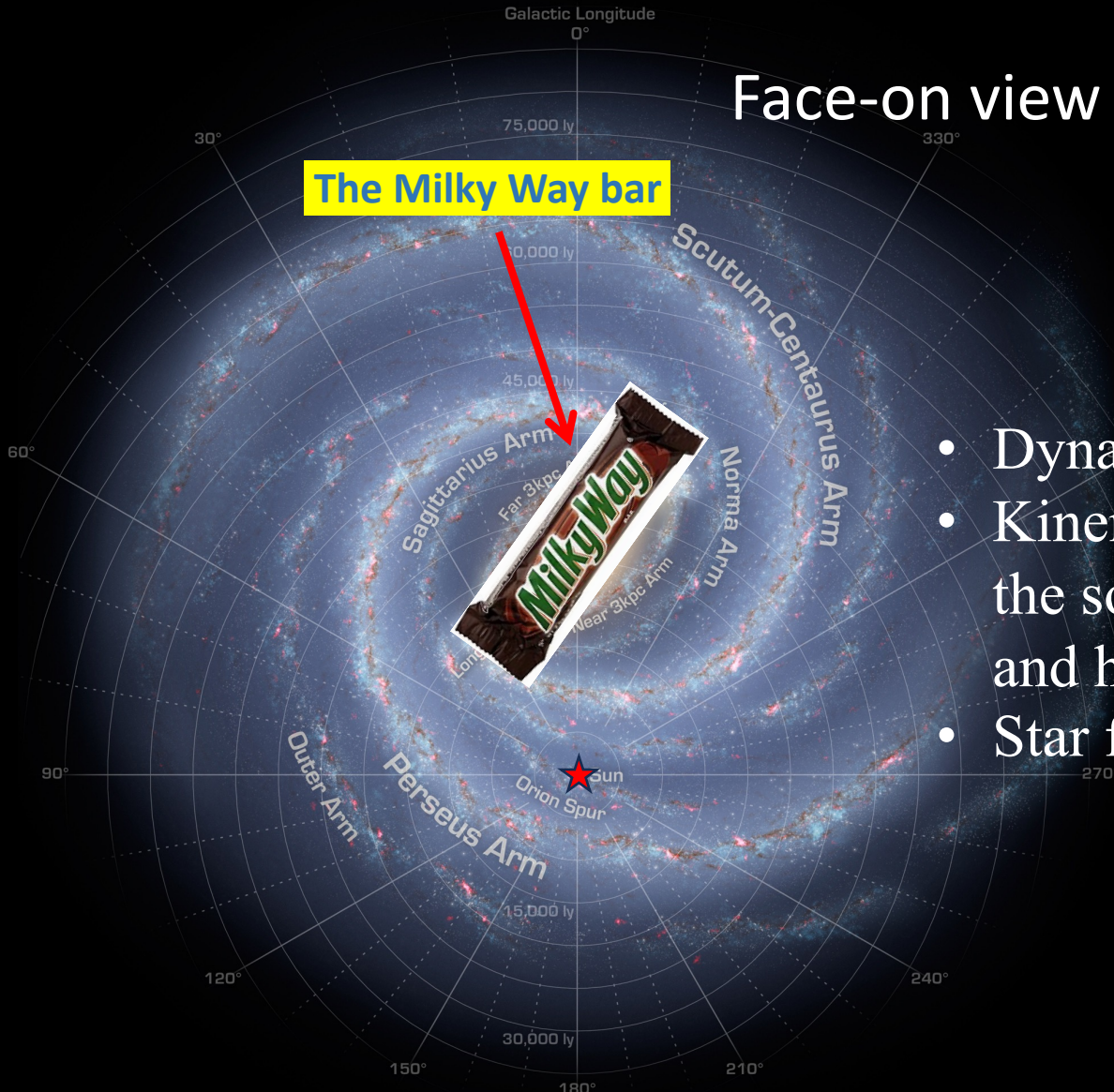


A panoramic photograph of the Galactic bar from long-period variables

Hanyuan Zhang (hz420@cam.ac.uk)

Collaborators: Vasily Belokurov, N. Wyn Evans, Jason L. Sanders, Zhao-Yu Li, Sarah G. Kane, Anke Ardern-Arentsen

Structures at the inner Galaxy

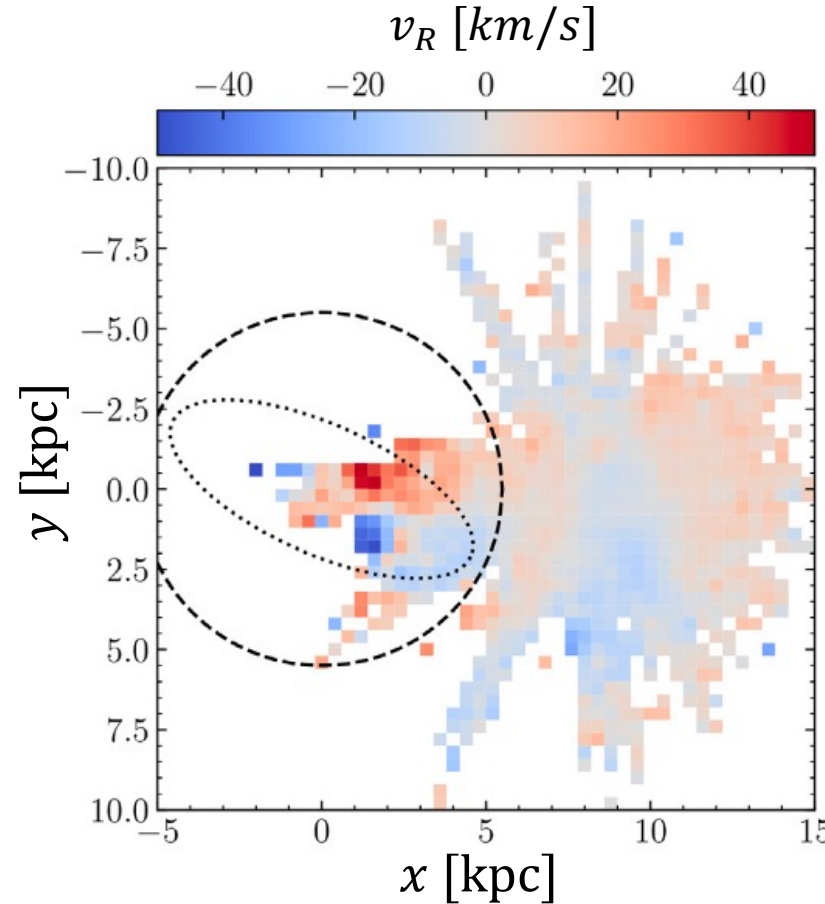


Face-on view

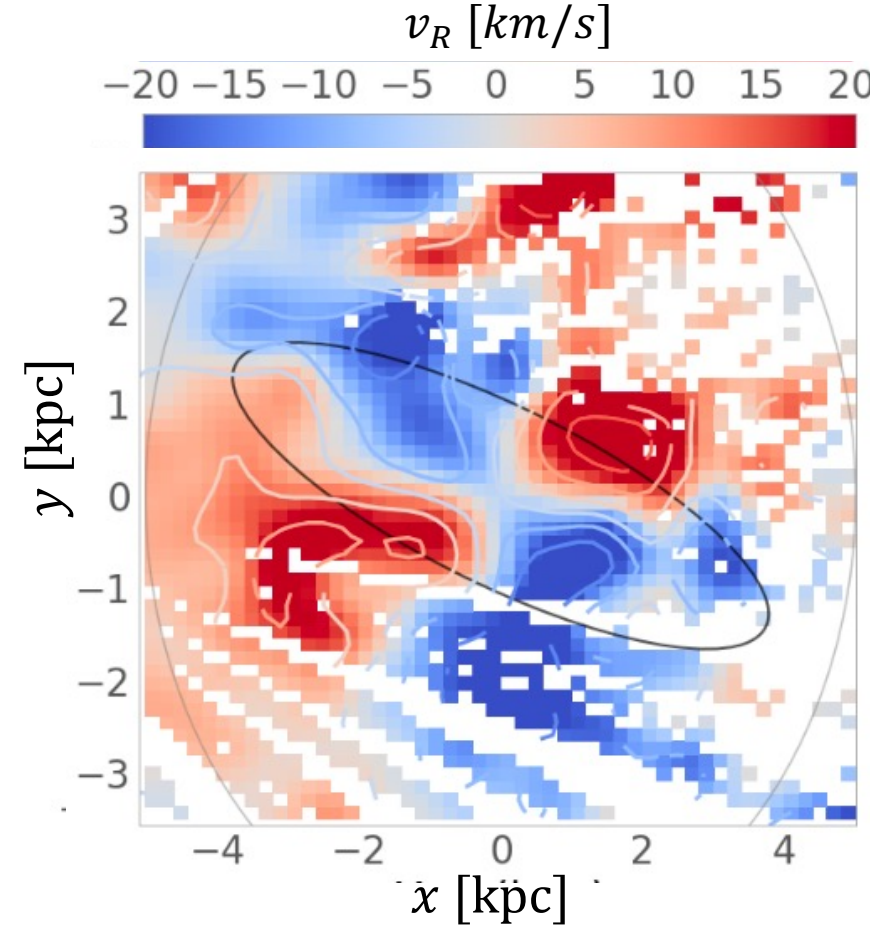
- Dynamics at the inner Galaxy
- Kinematic and equilibrium in the solar neighbourhood, disc, and halo
- Star formation history

Previous “photographs” of the Galactic bar:

Bovy+19, Queiroz+21 using spectroscopic distances



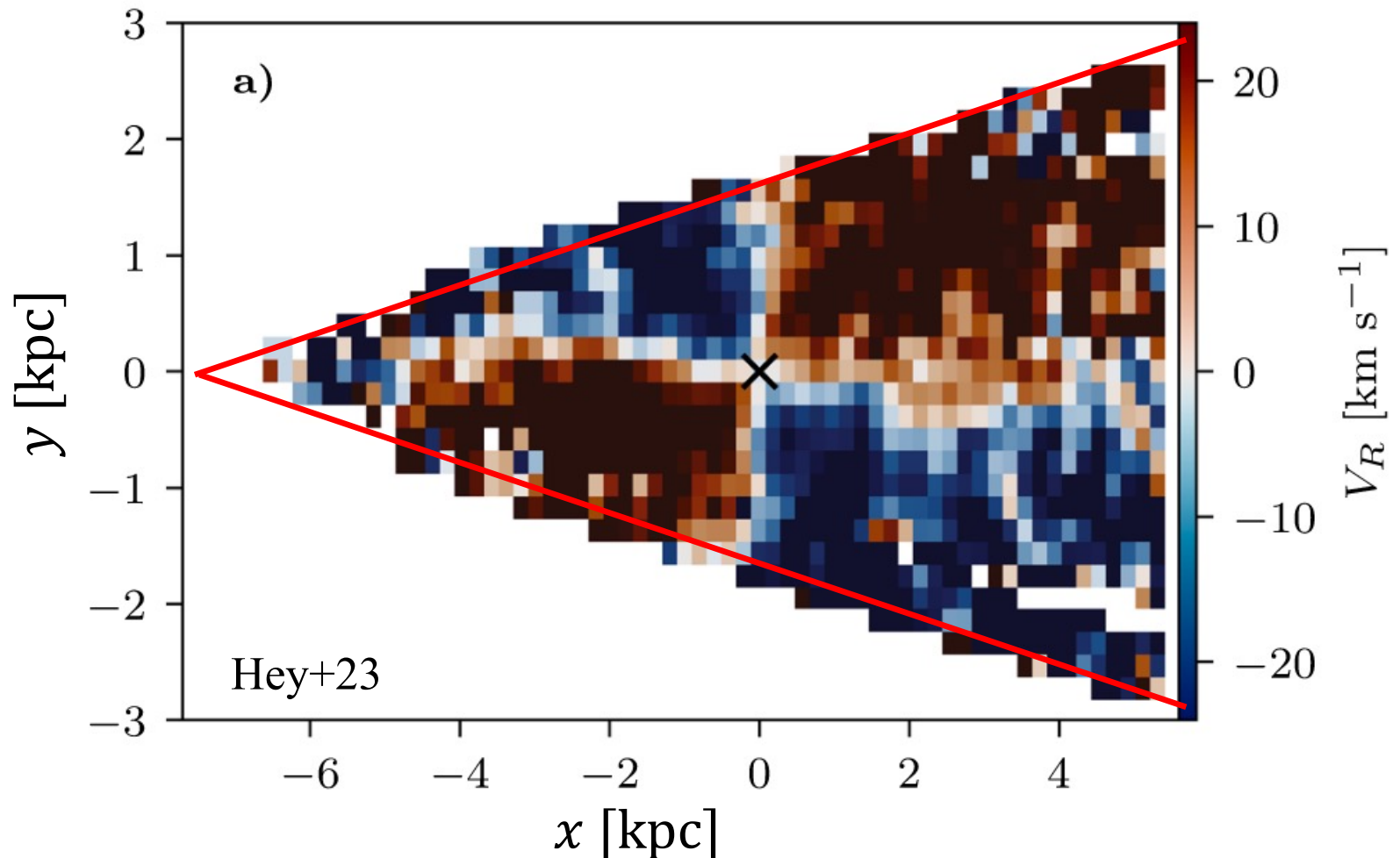
Bovy+19: APOGEE-AstroNN distances
Also see Leung+23 for an updated version



Queiroz+21 : APOGEE-StarHorse distances

Previous “photographs” of the Galactic bar:

Hey+23 using semi-regular variables in the OGLE survey

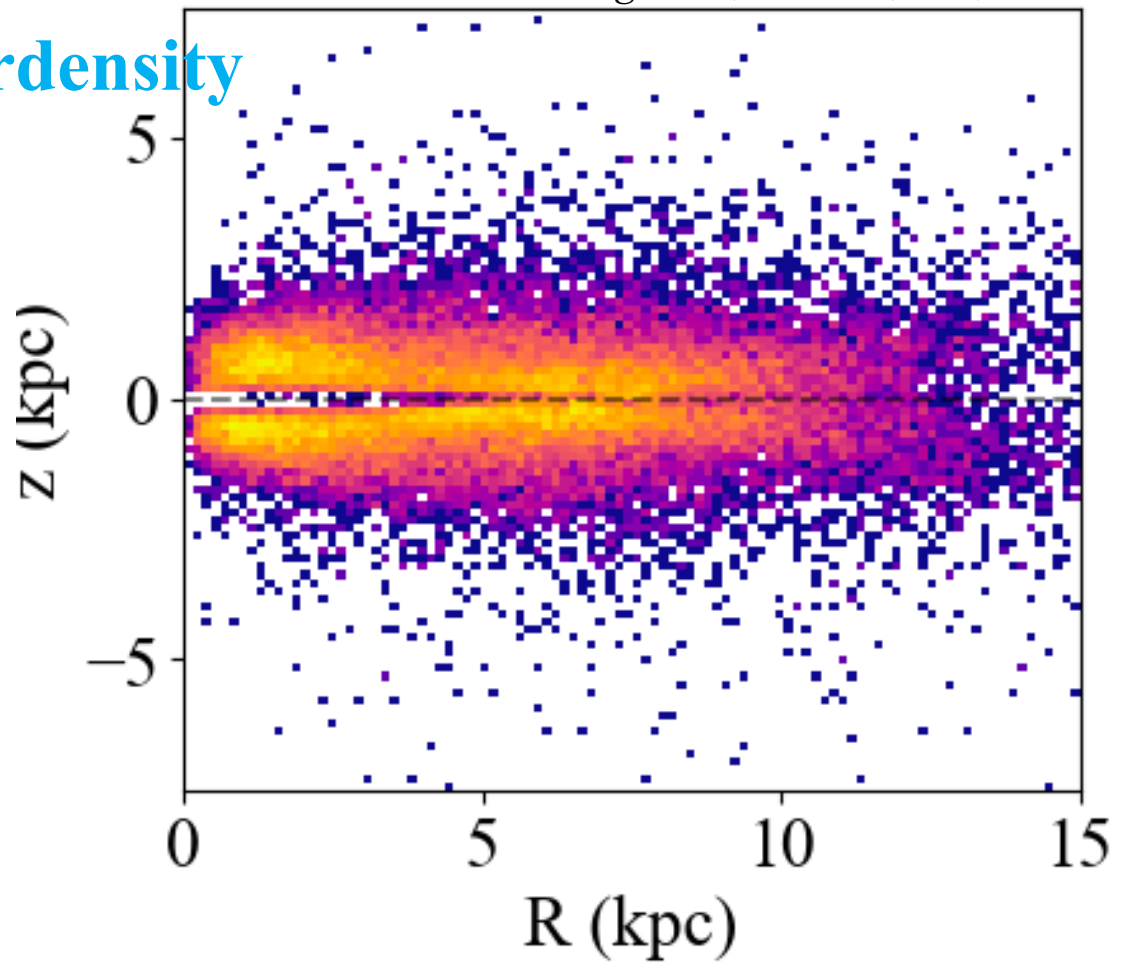
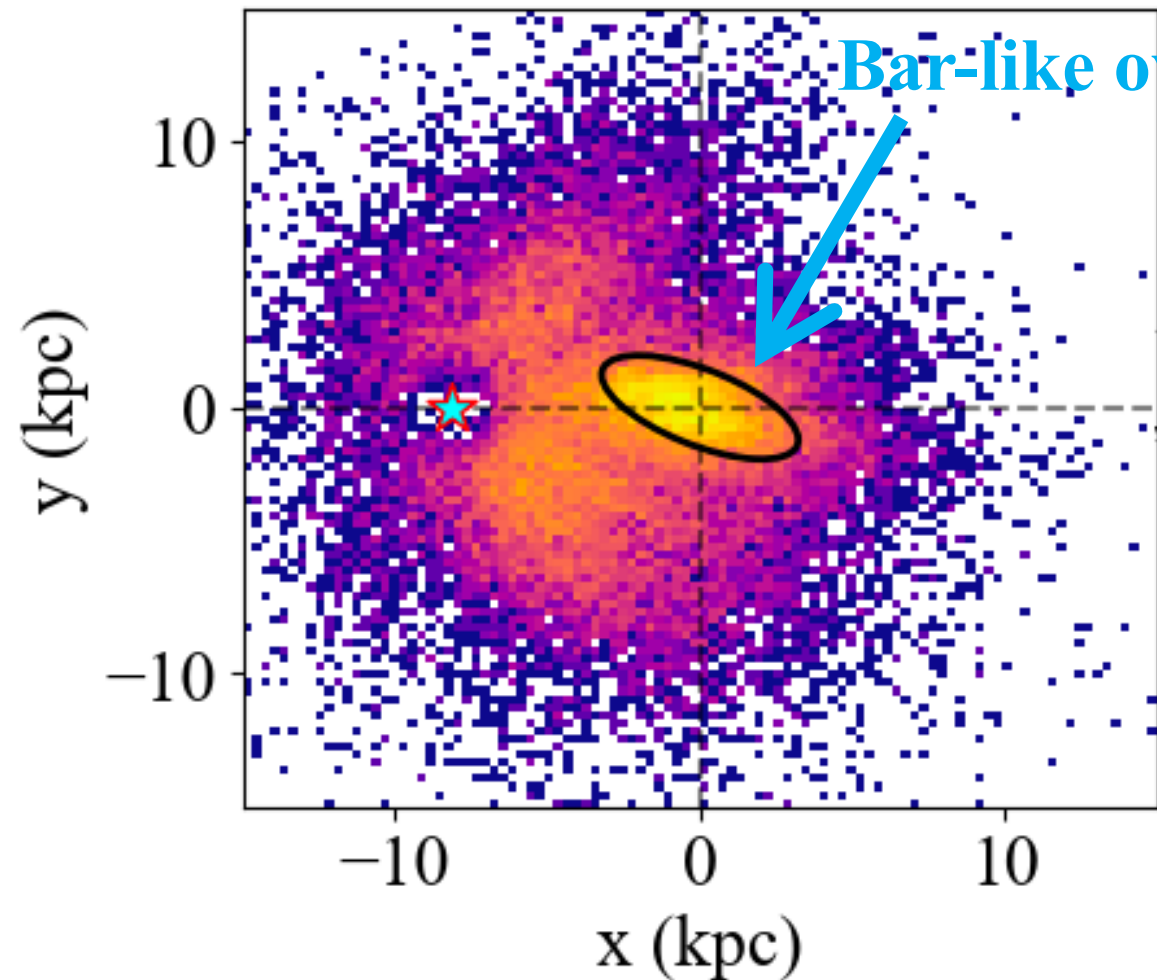


Low-amplitude, Long-period variable (LA-LPV)

- It is also called OGLE Small Amplitude Red Giants (OSARG)
- Long-period: $P \sim 10 - 100$ day (SRV and Mira usually have period ≥ 100 days)
- Smaller amplitude: $\Delta G \sim ? - 0.2$ mag (SRV and Mira usually have $\Delta G \geq 0.15$ mag)
- LA-LPV has compact period-luminosity relation resulting in a luminosity distance assignement with uncertainty of 10 – 15% (similar uncertainty to Mira and RRL)
- Better than Mira: LA-LPV has well measured line-of-sight velocity in Gaia DR3 already due to its smaller pulsation amplitude

Spatial distribution of LA-LPV in this sample

Zhang et al., MNRAS, 533, 3395–3414

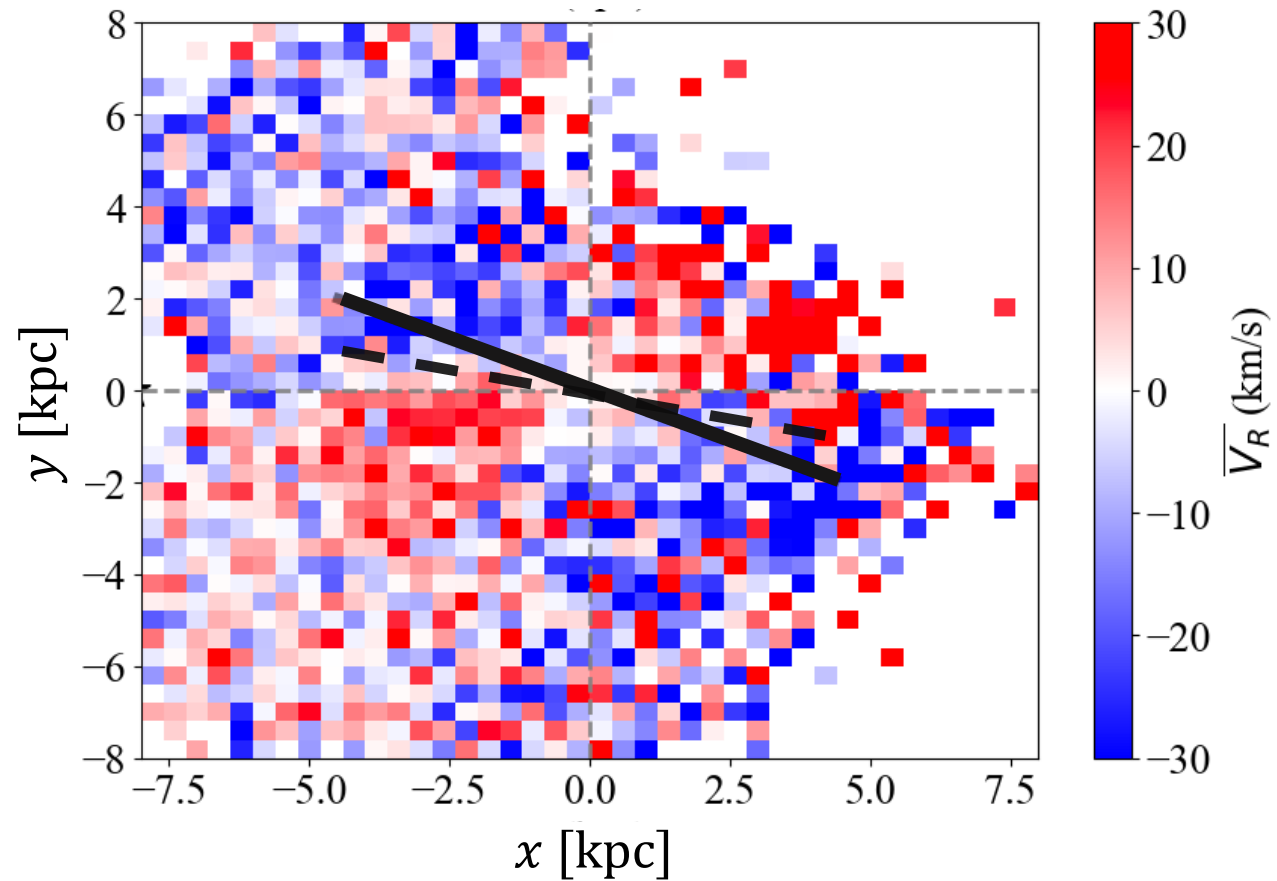


~34000 stars with full 6D phase space measurements & ~20000 are in the inner 5 kpc

Kinematics of the LA-LPV sample

Bar signature: Quadrupole v_R pattern

- Quadrupole pattern seen due to the streaming motion of the bar (Bovy+ 19)
- Sign-switching line biased towards the Sun-GC (Galactic centre) line due to the distance uncertainty (see Hey+23; Vislosky+24; Liao+24)

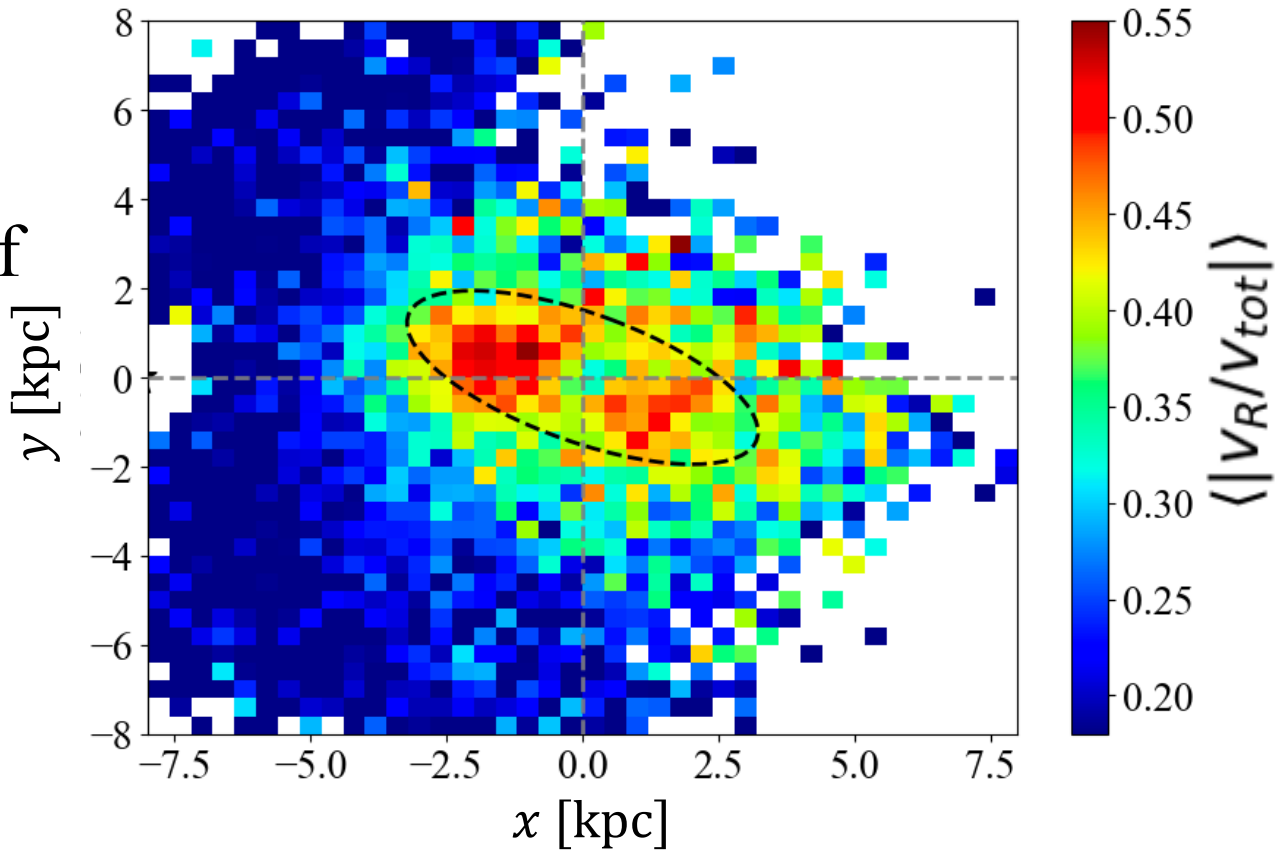


Kinematics of the LA-LPV sample

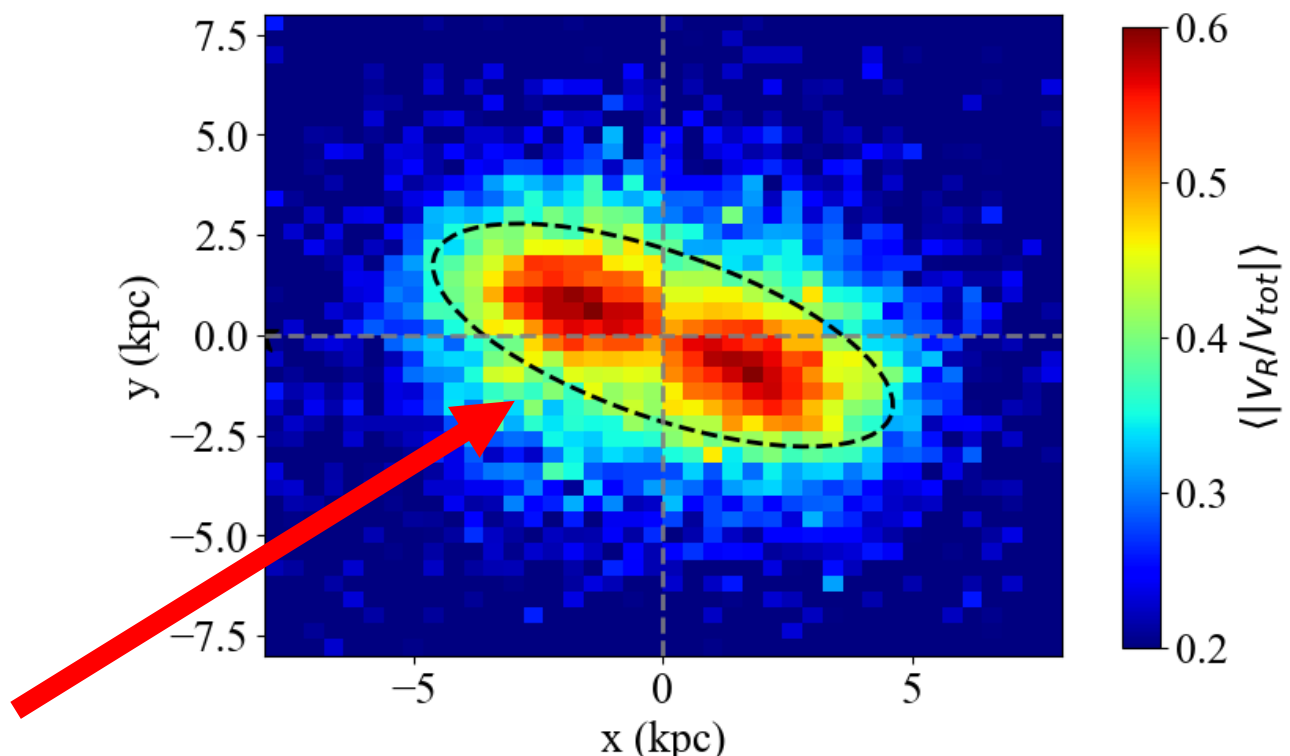
$$\left\langle \left| \frac{v_R}{v_{\text{tot}}} \right| \right\rangle = \frac{1}{N} \sum_j^N \frac{|v_{R,j}|}{v_{\text{tot},j}},$$

- High value is expected in the bar region due to the orbital structures of bar-supporting stars
- Less biased by the distance uncertainty as $\langle |v_R|/v_{\text{tot}} \rangle$ is a dimensionless quantity

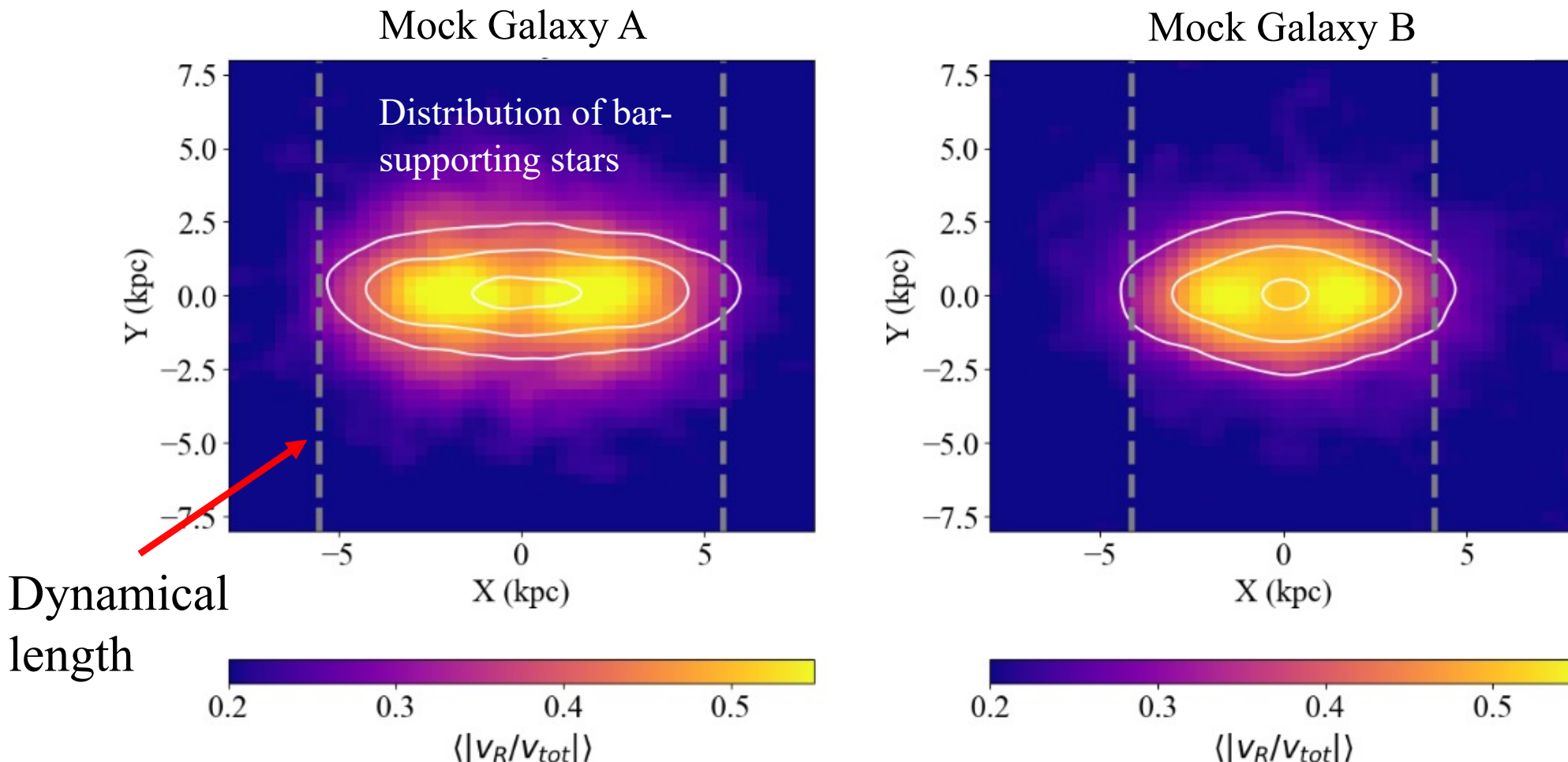
Bar signature: $\langle |v_R|/v_{\text{tot}} \rangle$ map



$|v_R/v_{tot}|$ map in a N-body simulated Galaxy



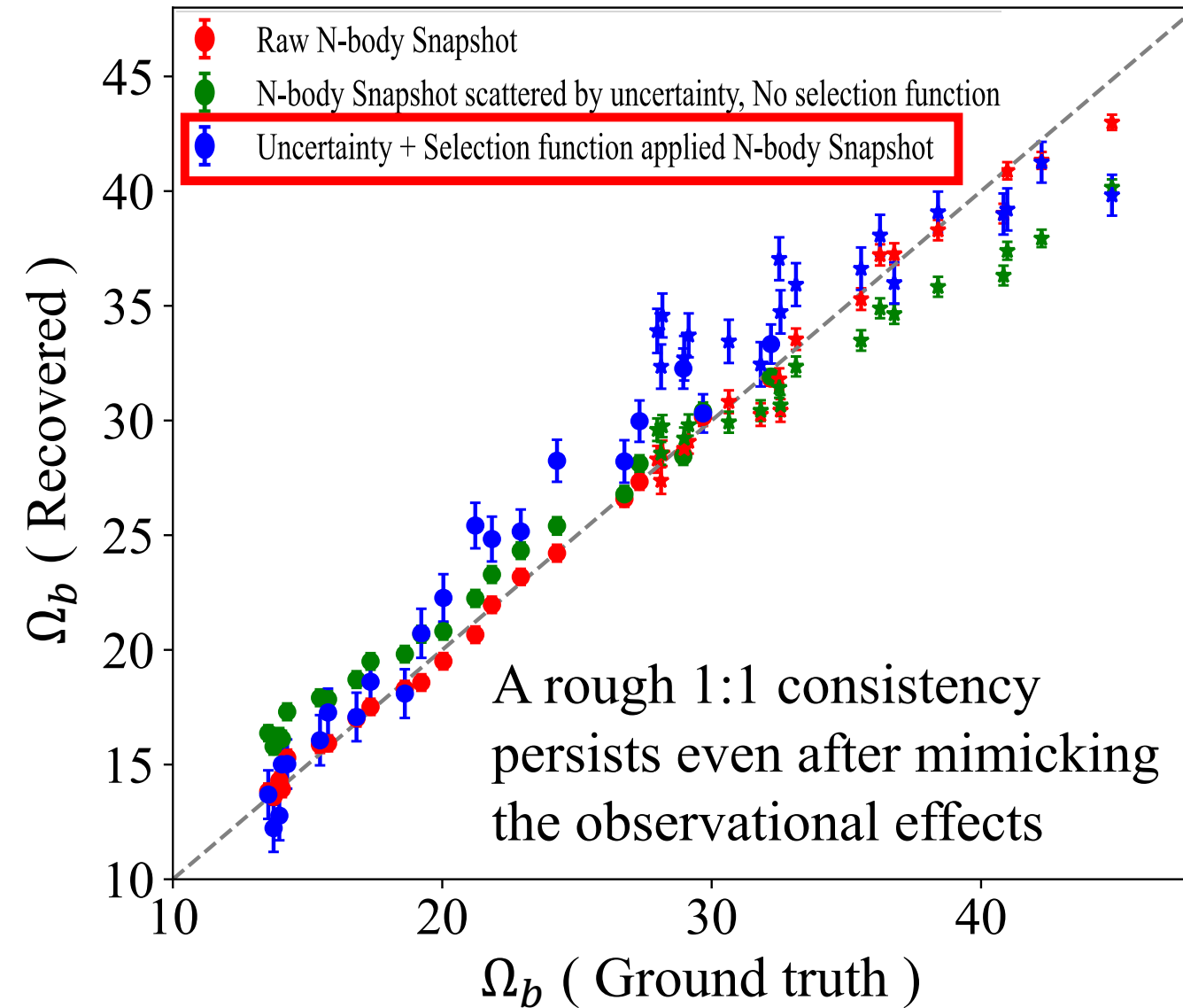
$|v_R/v_{tot}|$ map as a tracer of the bar-supporting stars



- Bar-supporting stars distributed similarly to the signal in the $|v_R/v_{tot}|$ map
- Can be used as an estimator of the dynamical length of the MW bar → 4.0 kpc

Also see Petersen+24 for a similar method that is applicable for extragalactic observations

Estimation of the pattern speed using Dehnen+23's method



Designed for simulation;
Introducing distance uncertainty and
selection function typically lead to bias

Apply to the LA-LPV sample

$$\Omega_b \sim 34.1 \pm 2.4 \text{ km s}^{-1} \text{kpc}^{-1}$$

for the Milky Way bar

Consistent to other observations using
different methods (see Dillamore+23,24;
Clarke&Gerhard 22, etc.)

Timing the Galactic disc formation through bar chrono-kinematics

2) Zhang et al. 2024, submitted,
arxiv:2408.16815

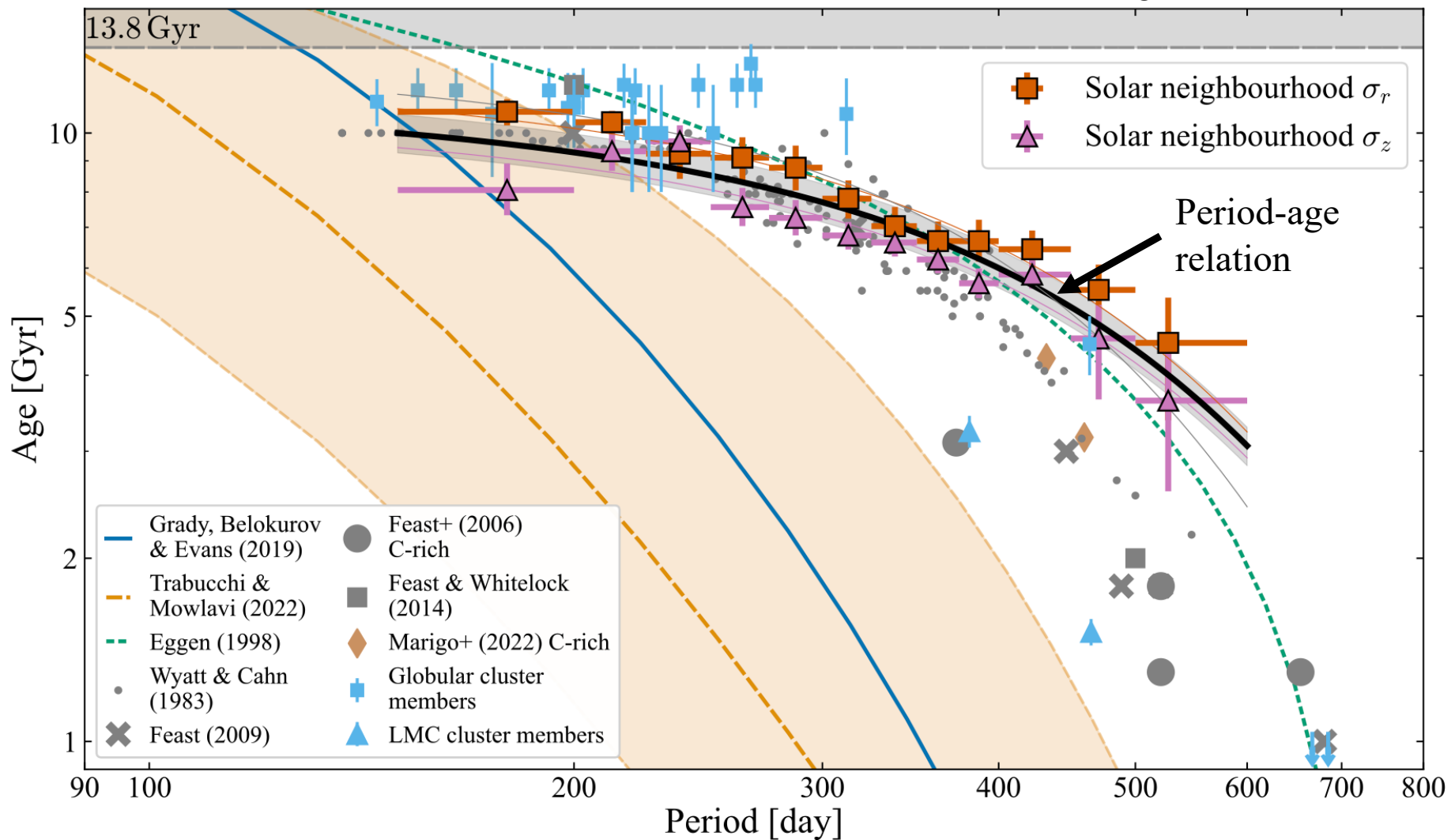


Deciphering the Milky Way disc formation time encrypted in the chrono-kinematics of the bar

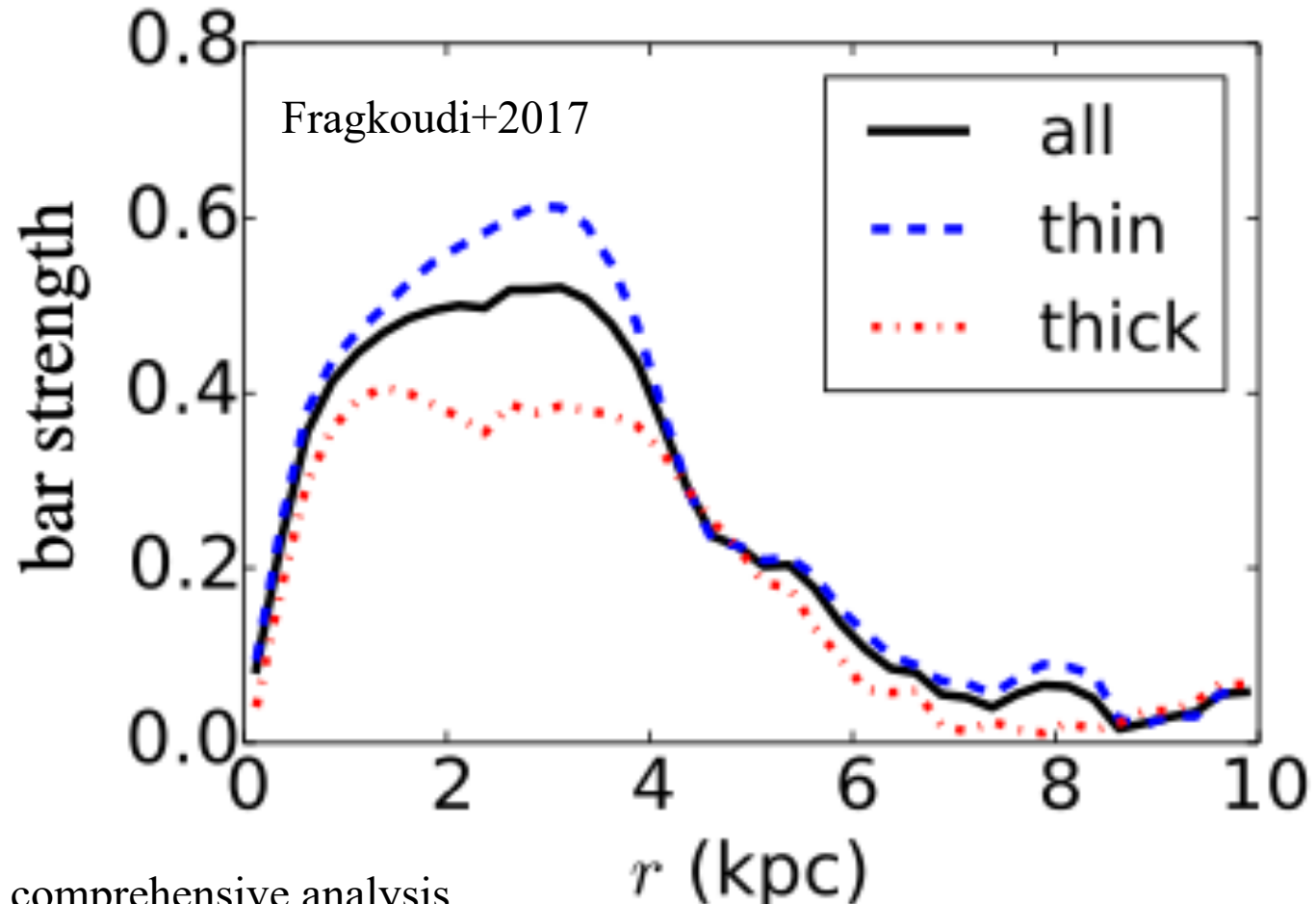
Hanyuan Zhang¹  , Vasily Belokurov¹ , N. Wyn Evans¹ , Zhao-Yu Li^{2,3} , Jason L. Sanders⁴  and Anke Ardern-Arentsen¹ 

Ingredient 1: Period-age relation of Mira variables

Zhang & Sanders 2023



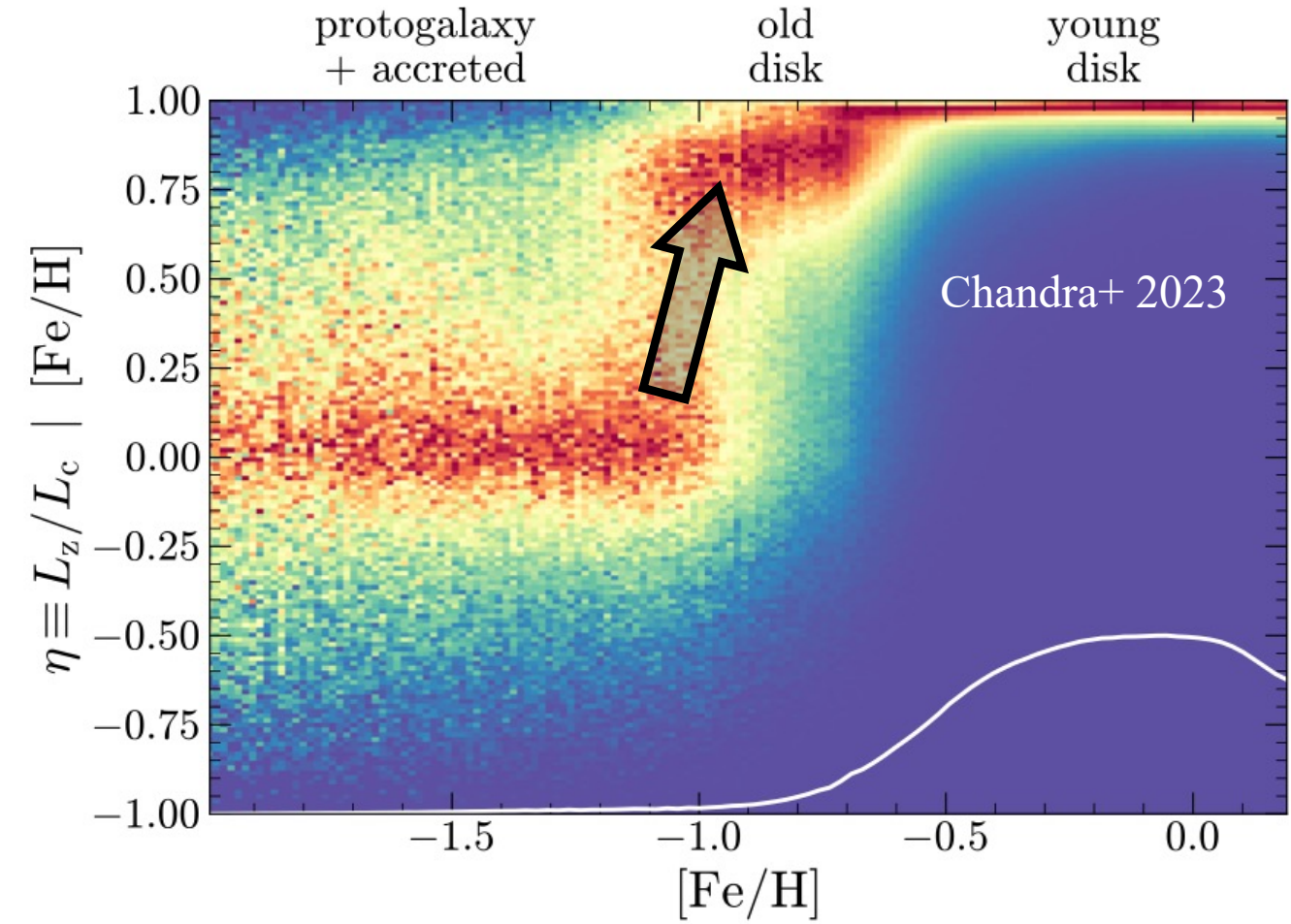
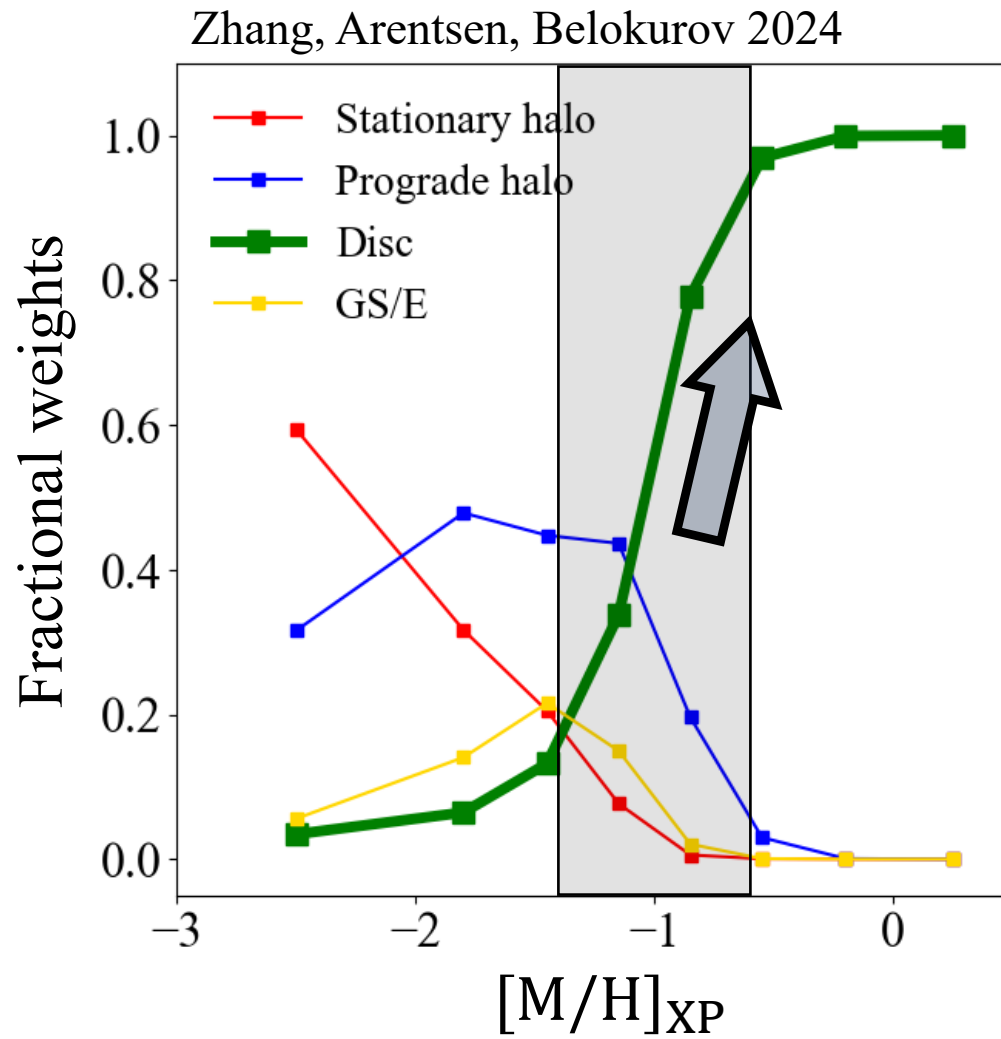
Ingredient 2: Kinematically cold stars response more actively to the bar



See Debattista+17 for a more comprehensive analysis

See also Di Matteo+15 & 19 and Ness+13 for a more evidence on bar constituents and inner Galactic kinematics with different metallicities

Ingredient 3: Rapid disc formation of the Milky Way

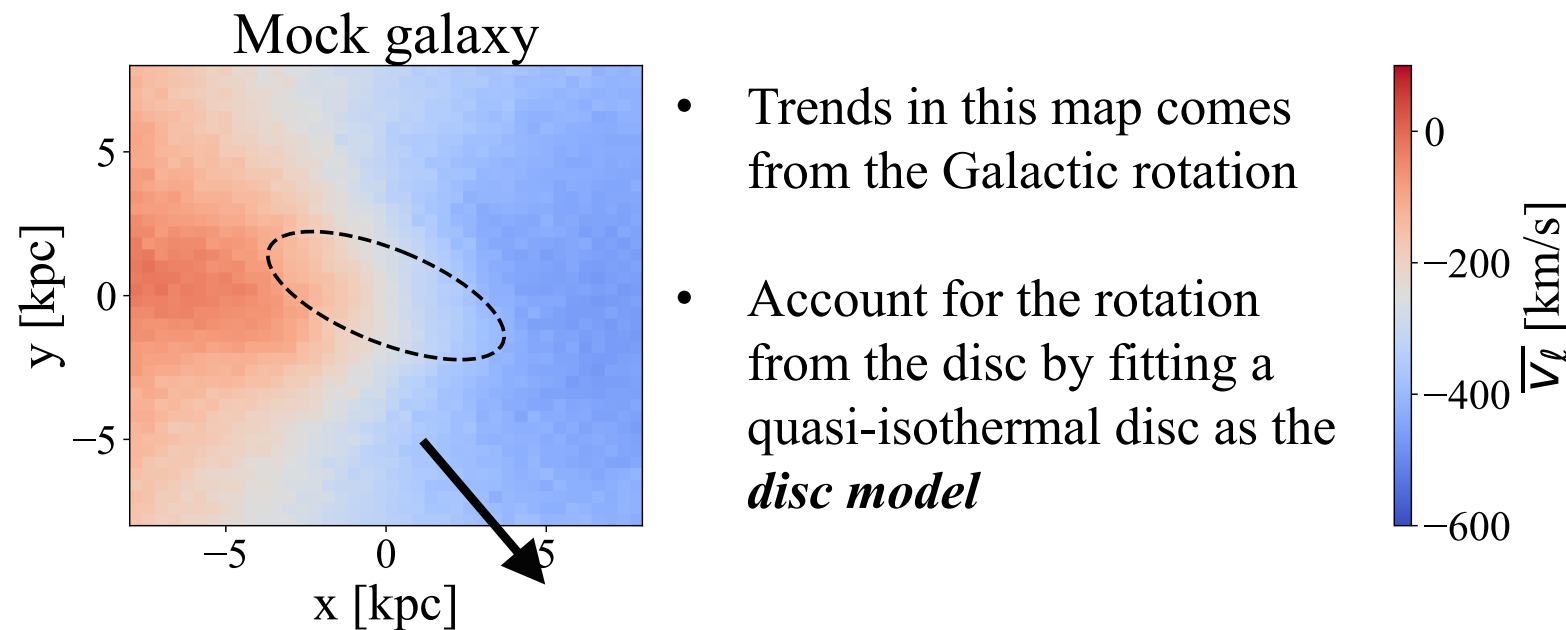


See also Belokurov & Kravtsov 22 & 24 for more observation evidence and Dillamore+ 2024 for simulation

Δv_l map as a tracer of bar signatures: N-body galaxy

Velocity in the Galactic longitude direction
i.e. $v_l = 4.74 \mu_l \times d$

Although v_l is the velocity in a heliocentric coordinate, it still embed the information on the *Galactic rotation* as it is an in-plane velocity

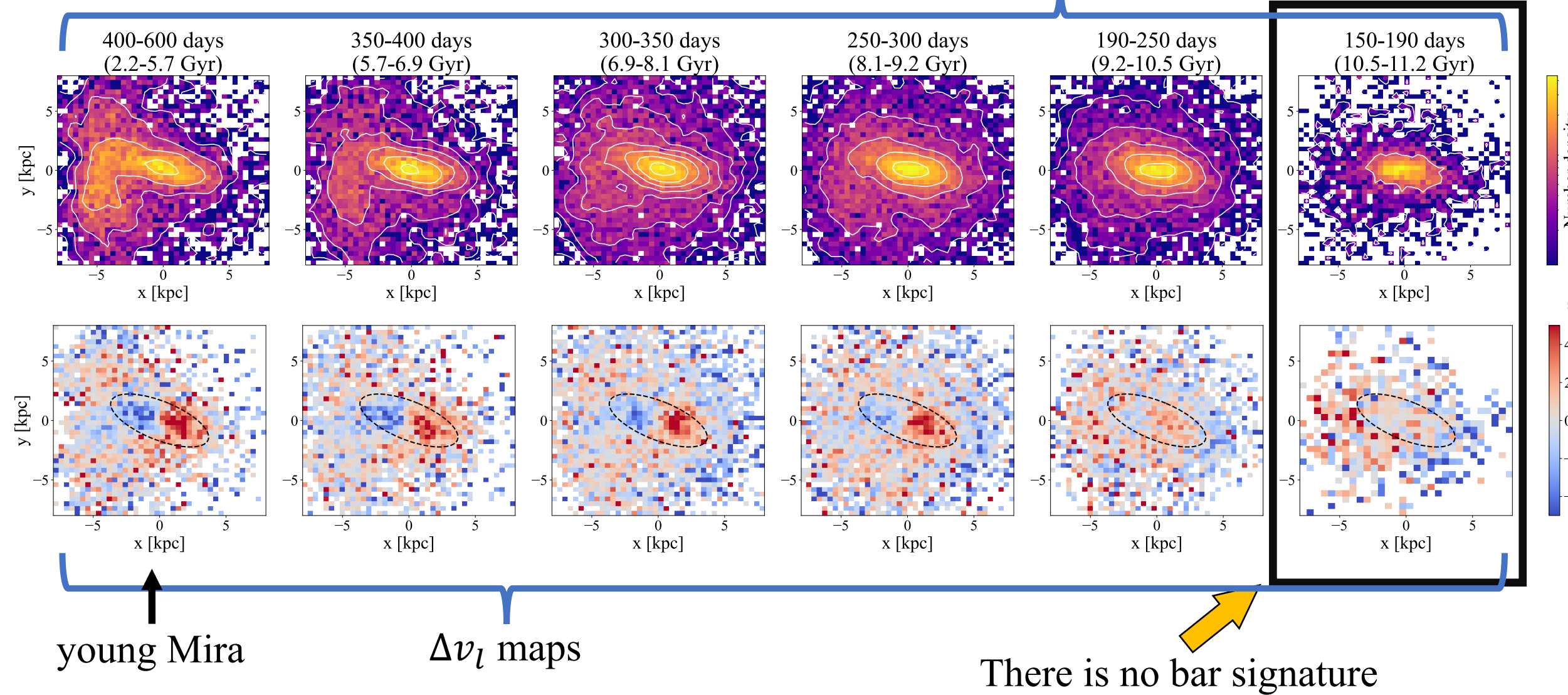


Dipole-like signature caused by the bar

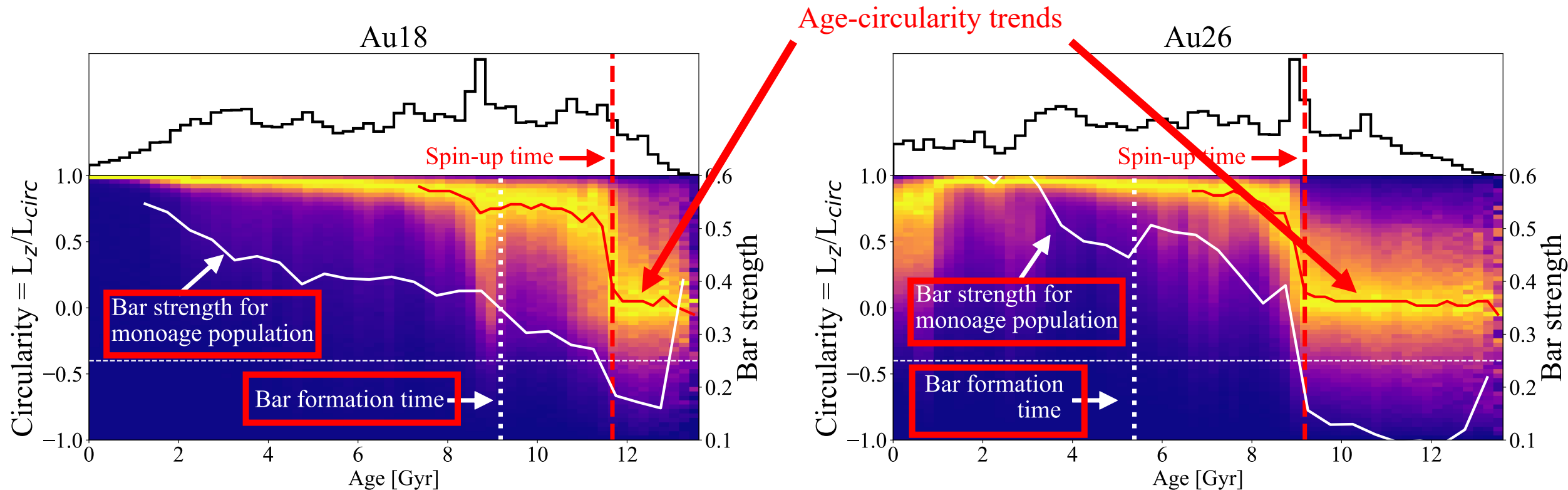
Bar chrono-kinematic from Mira variables

See also Grady+20, Semczuk+22 for age-morphology trends

Stellar surface density



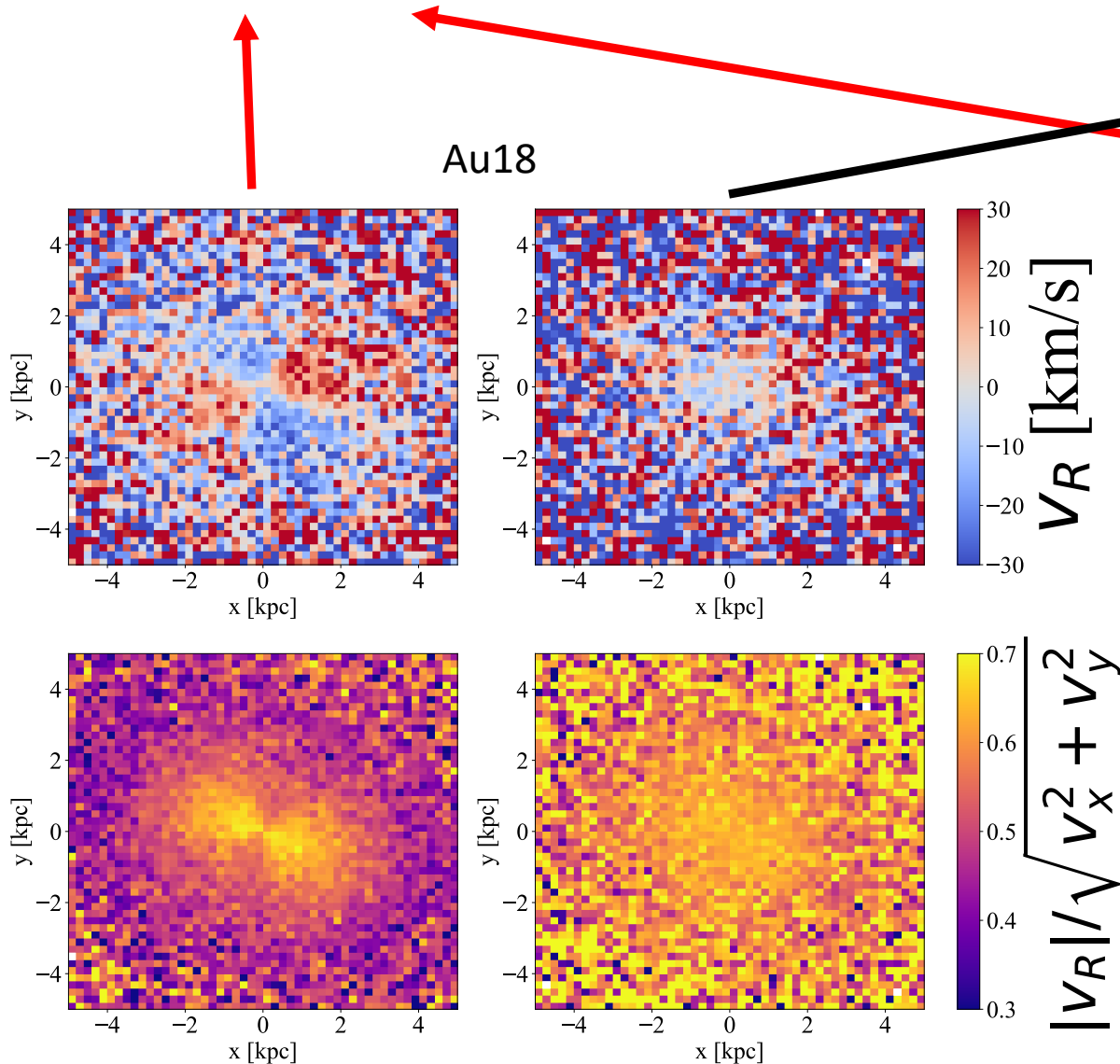
Auriga cosmological simulations: Spin-up in Au18 & Au26 and its relation to bar strength



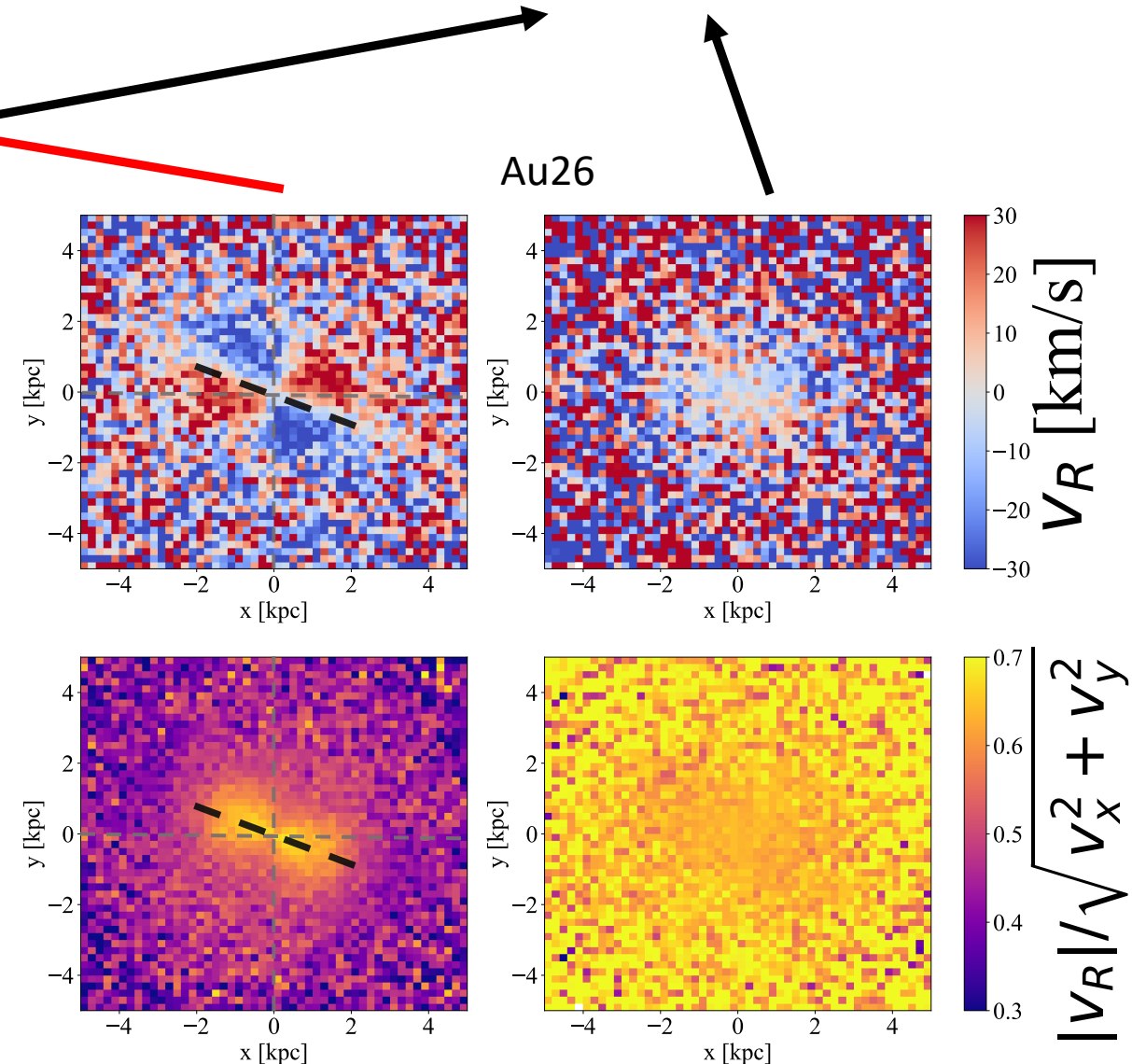
Bar signature appears for population born right after the disc formation because:

- the disc formation was rapidly so that disc population quickly dominate over the halo stars
- the disc population born after the spin-up (but before bar formation) are captured by the bar and show bar signatures at the present-day

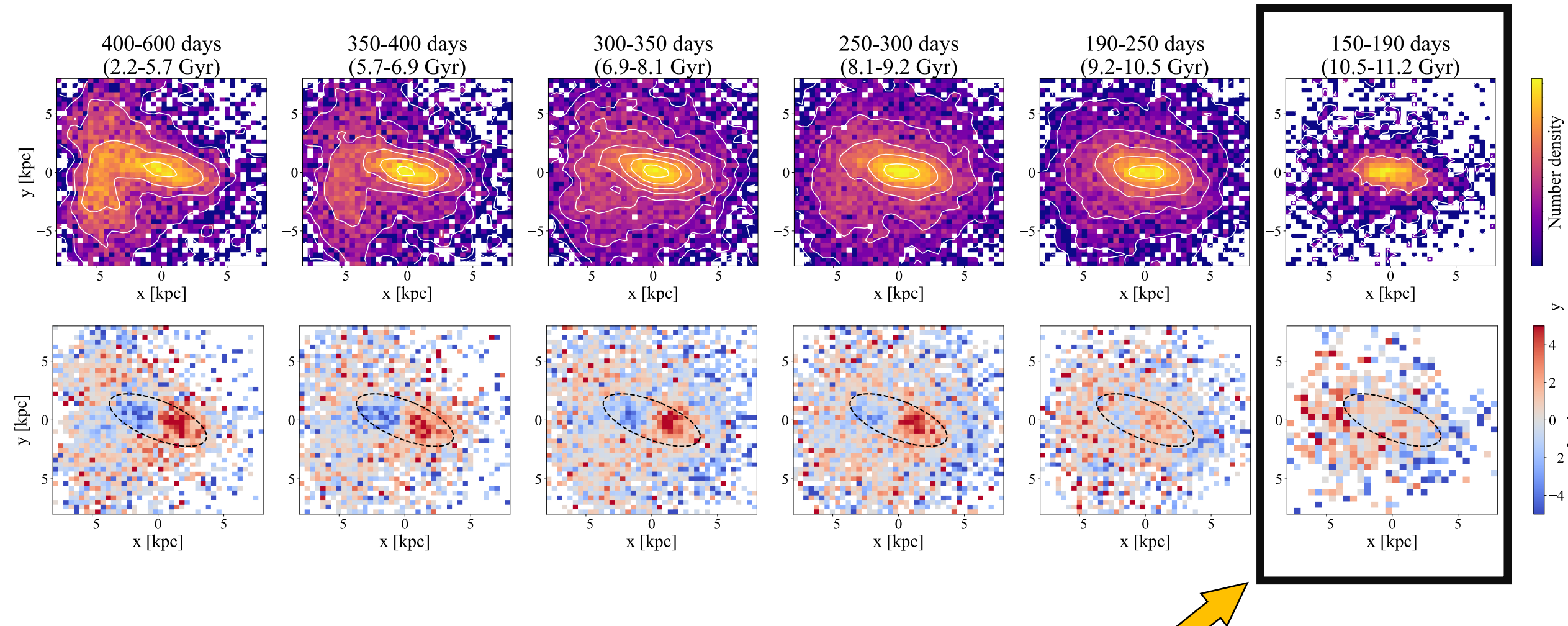
Population born within
1Gyr *after* the spin-up



Population born within
1Gyr *before* the spin-up



Bar chrono-kinematic from Mira variables



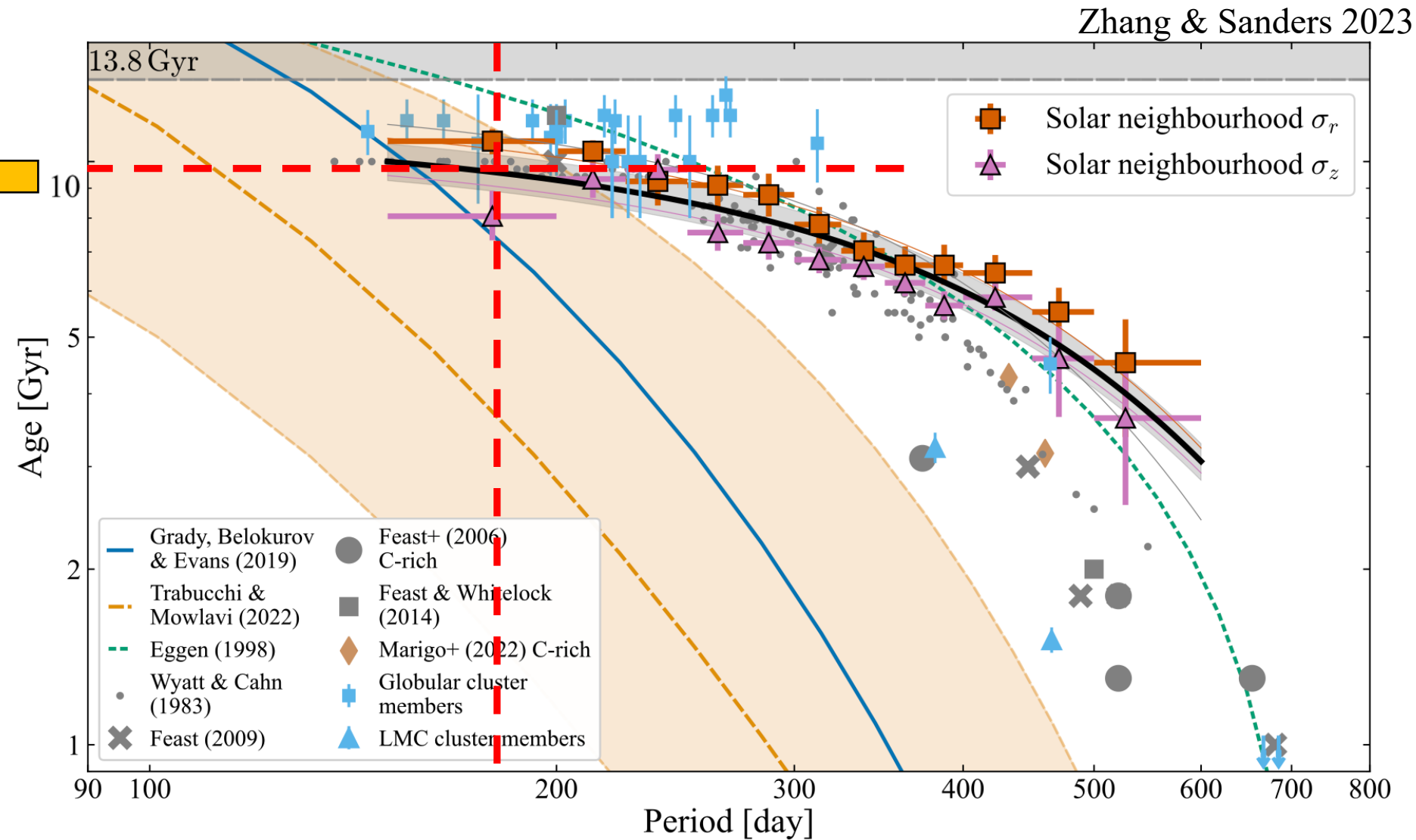
There is no bar signature

Constrain on the Galactic spin-up time

Mira with period around 190 days

10.5 ± 1.2 Gyr

A disc younger than 12 Gyr



Summary:



- With LA-LPV:

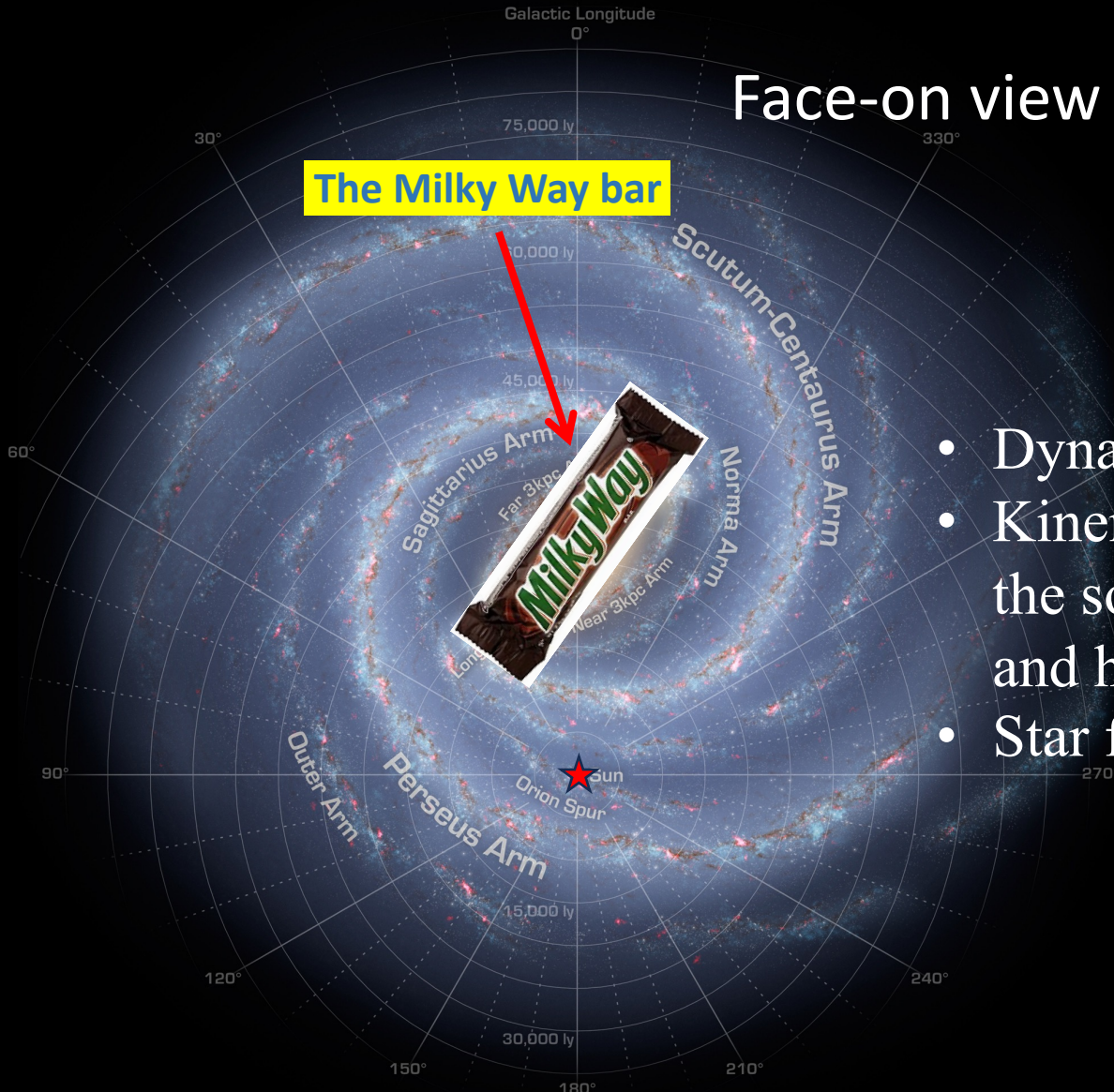
- Kinematic maps (v_R and $|v_R/v_{tot}|$ map) of the inner Galaxy with minimal spatial selection function and large coverage – LA-LPV is a good kinematic tracer to map the inner Galaxy
- $|v_R/v_{tot}|$ map can trace the bar-supporting stars and hence can be used to estimate the dynamical length of the Milky Way bar: $R_b \sim 4.0$ kpc
- We calculate the pattern speed of the Galactic bar $\Omega_b \sim 34.1 \pm 2.4$ km s⁻¹kpc⁻¹ using the pattern speed estimator developed in Dehnen+23

- With Mira:

- We demonstrate the correlation between the disc chrono-kinematics and bar chrono-kinematics using Auriga simulations, and proposed to use that to measure the disc formation time
- We trace the chrono-kinematic signature of the inner Galaxy and find no bar signature for Mira with period shorter than 190 days (Age $\sim 10.5 \pm 1.2$ Gyr)
- Therefore, we can constrain the Milky Way's disc to be younger than ~ 12 Gyr



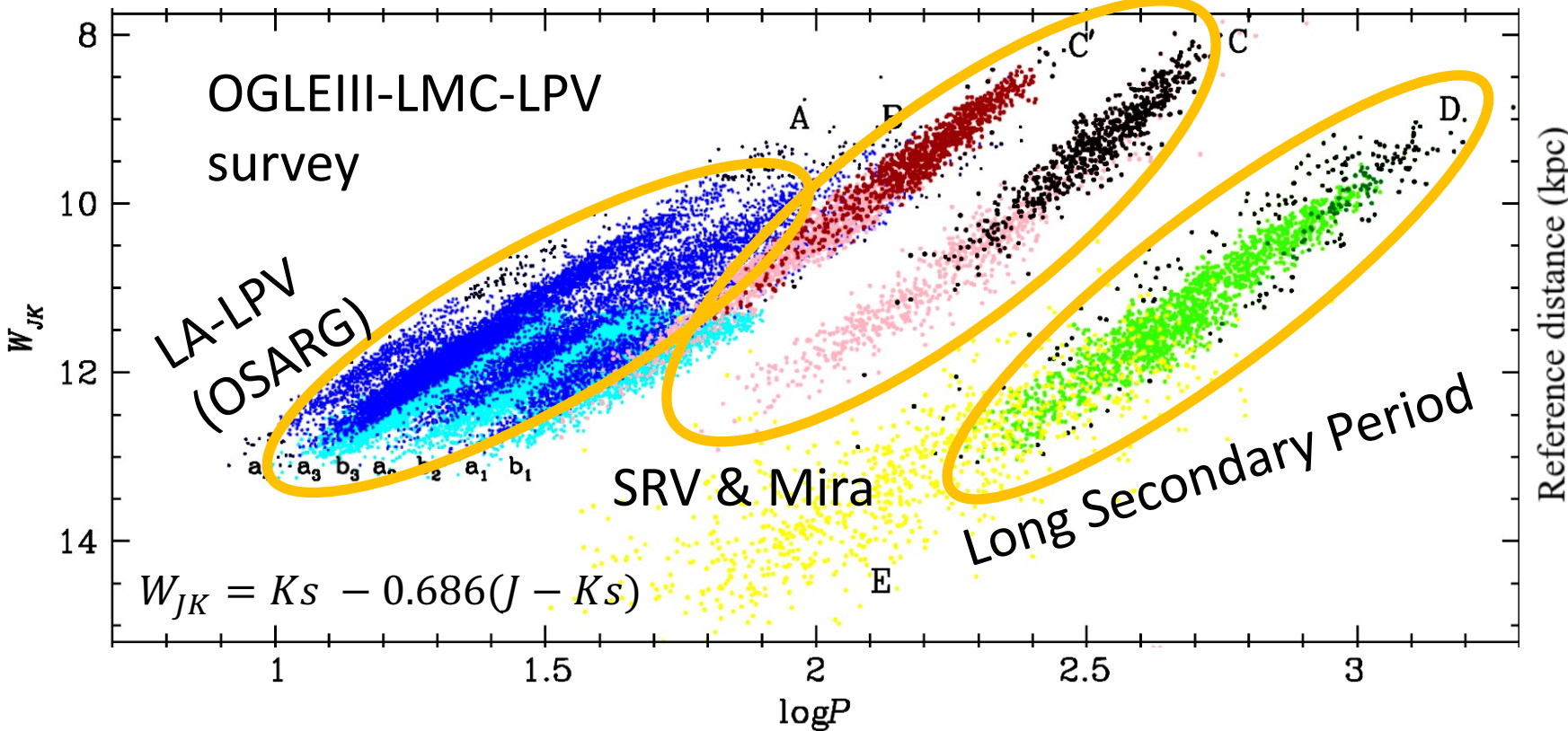
Structures at the inner Galaxy



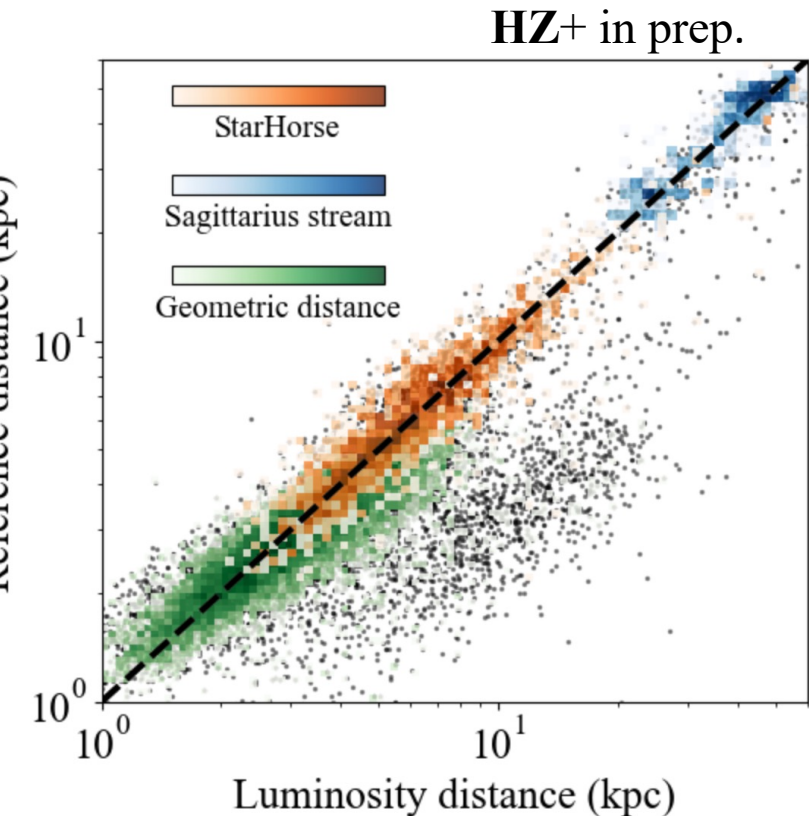
Face-on view

- Dynamics at the inner Galaxy
- Kinematic and equilibrium in the solar neighbourhood, disc, and halo
- Star formation history

LA-LPV as distance indicators



Soszynski+07

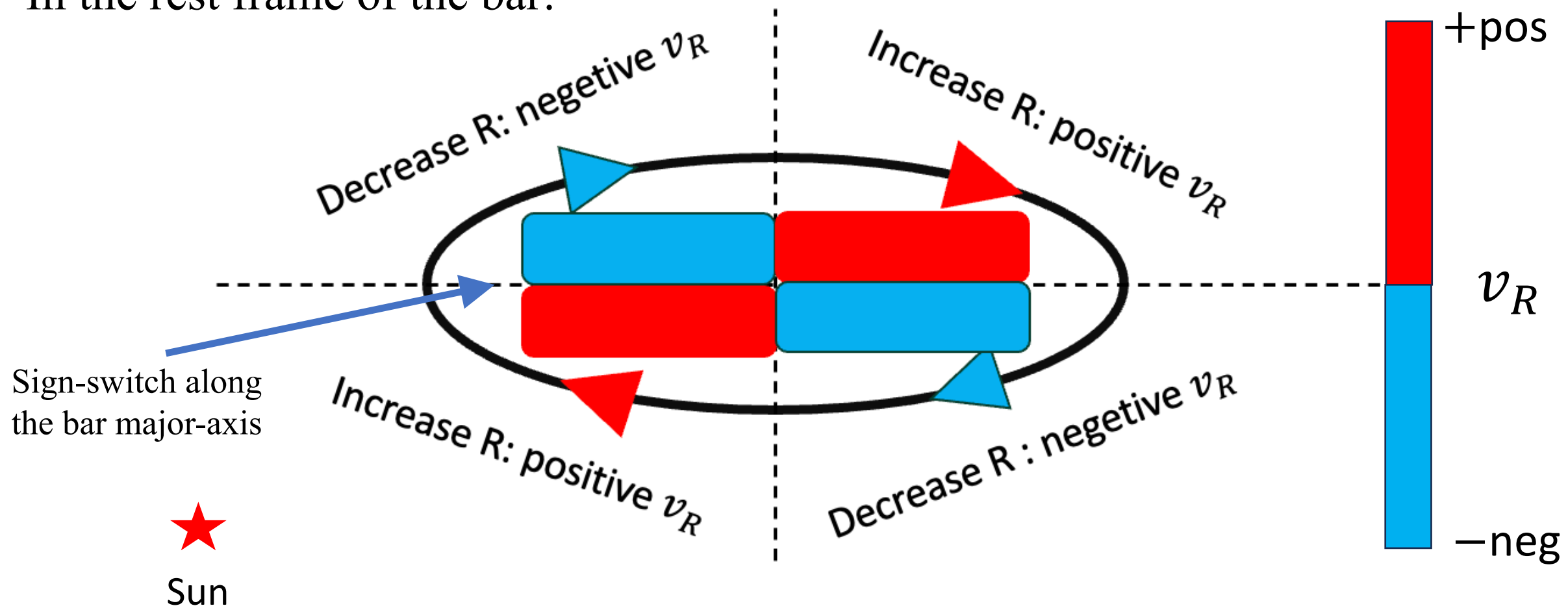


$$\sigma_d \sim 10 - 15\%$$

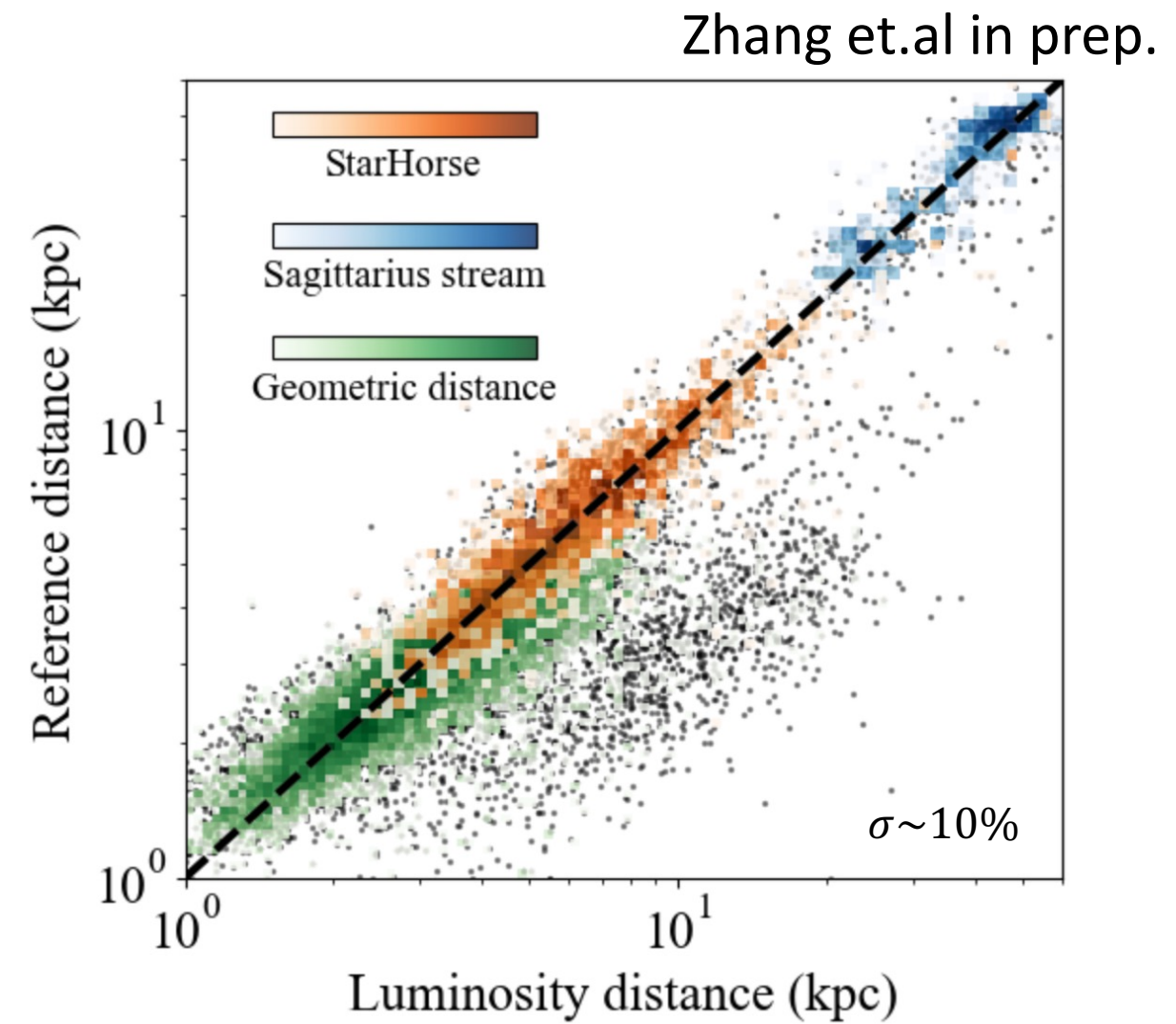
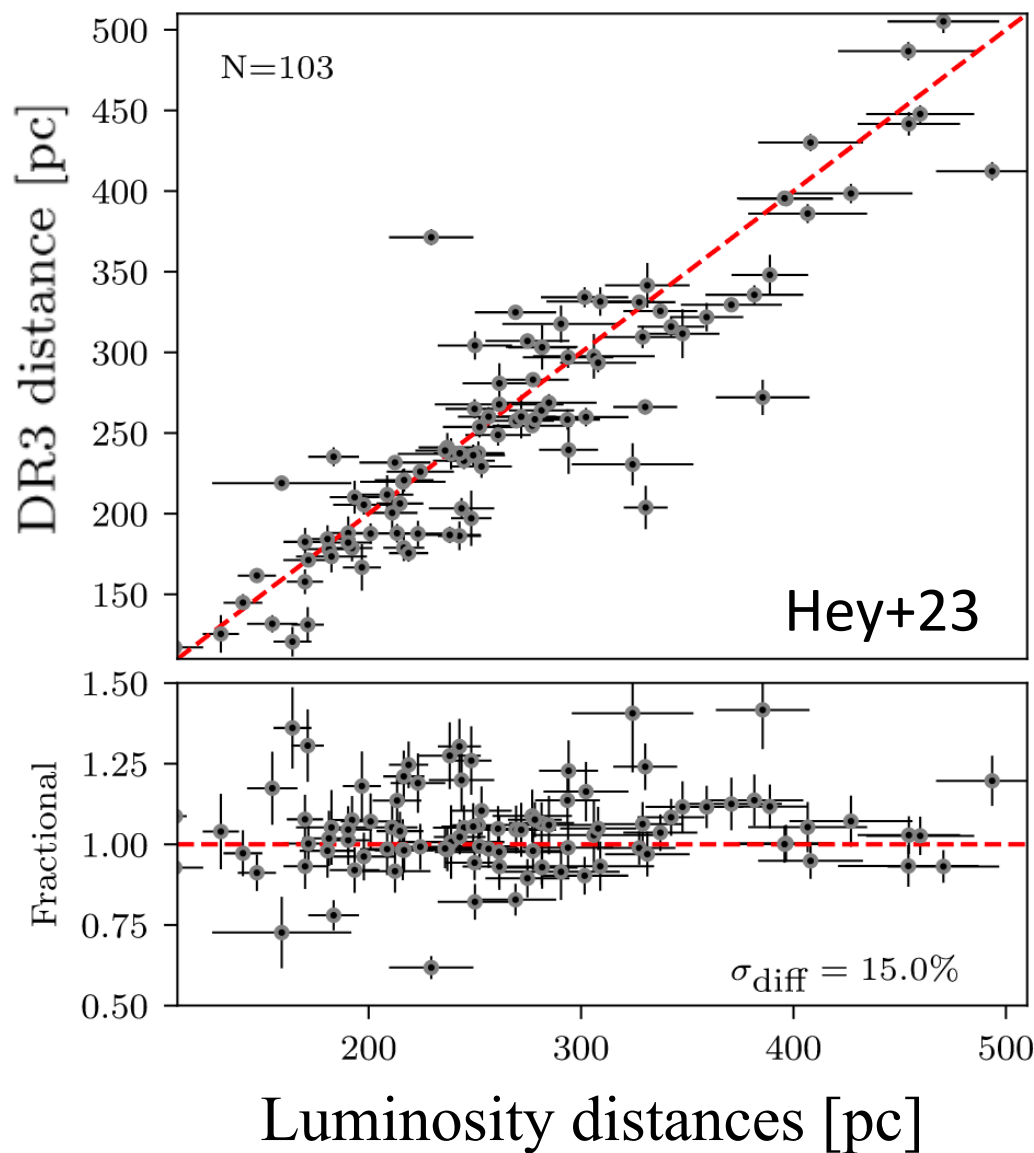
Kinematic signature of the bar:

Quadrupole pattern in v_R

In the rest frame of the bar:

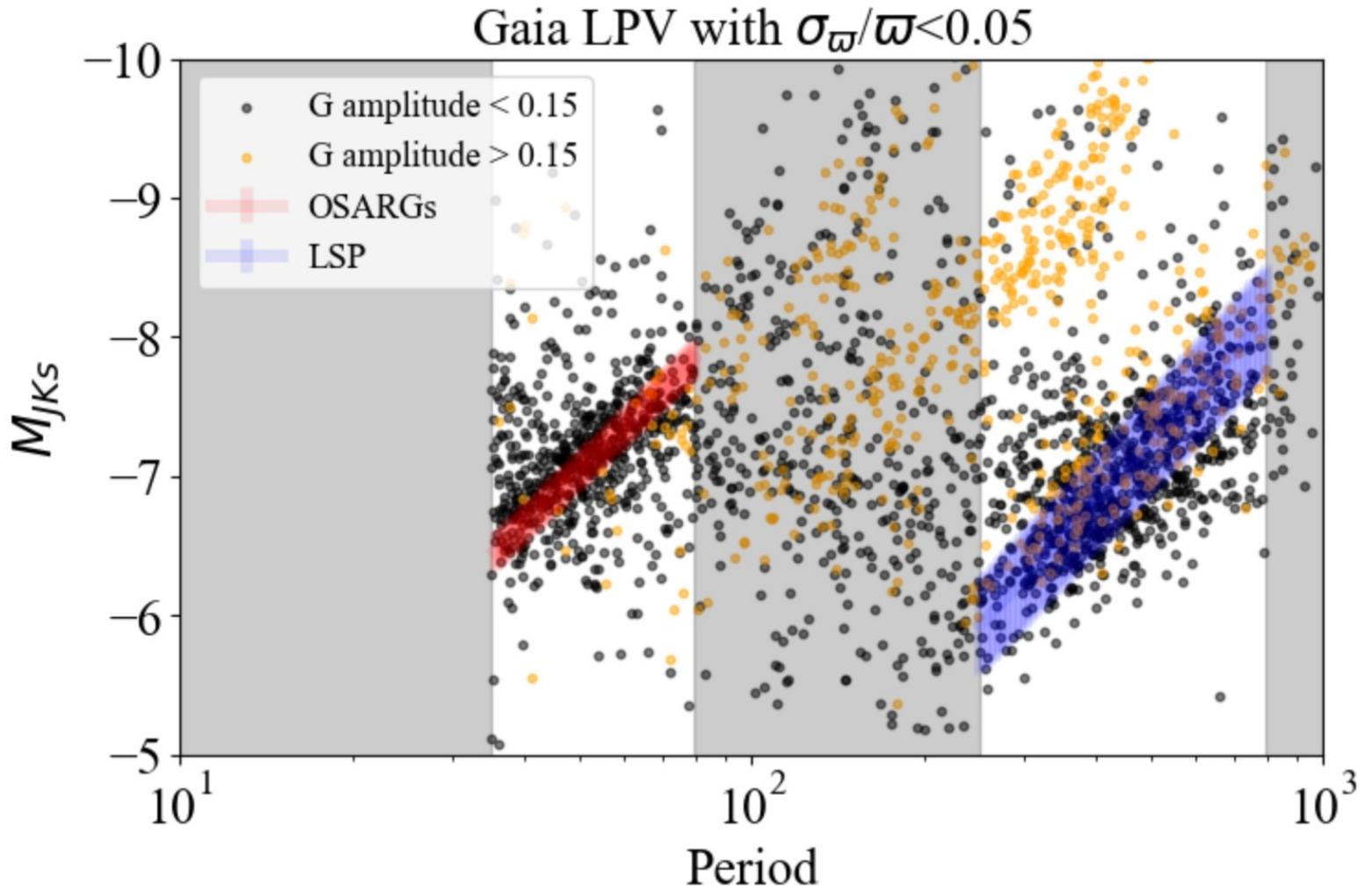


The accuracy and precision of the luminosity distances

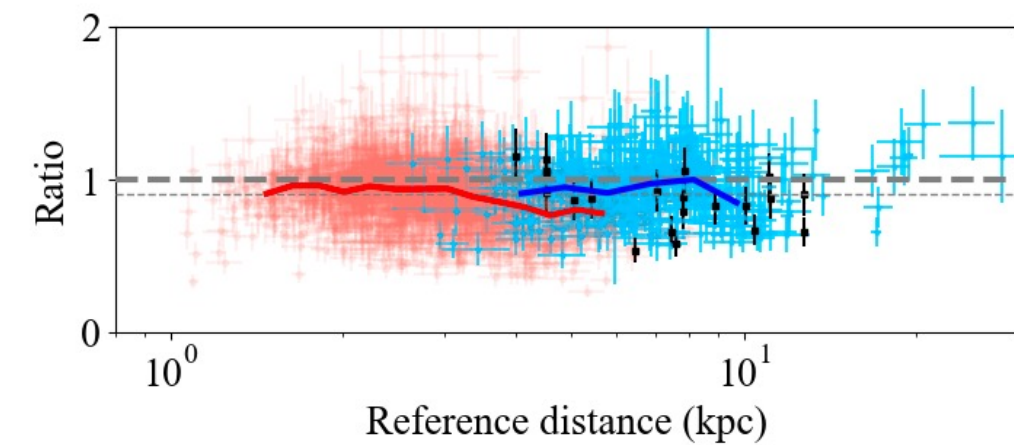
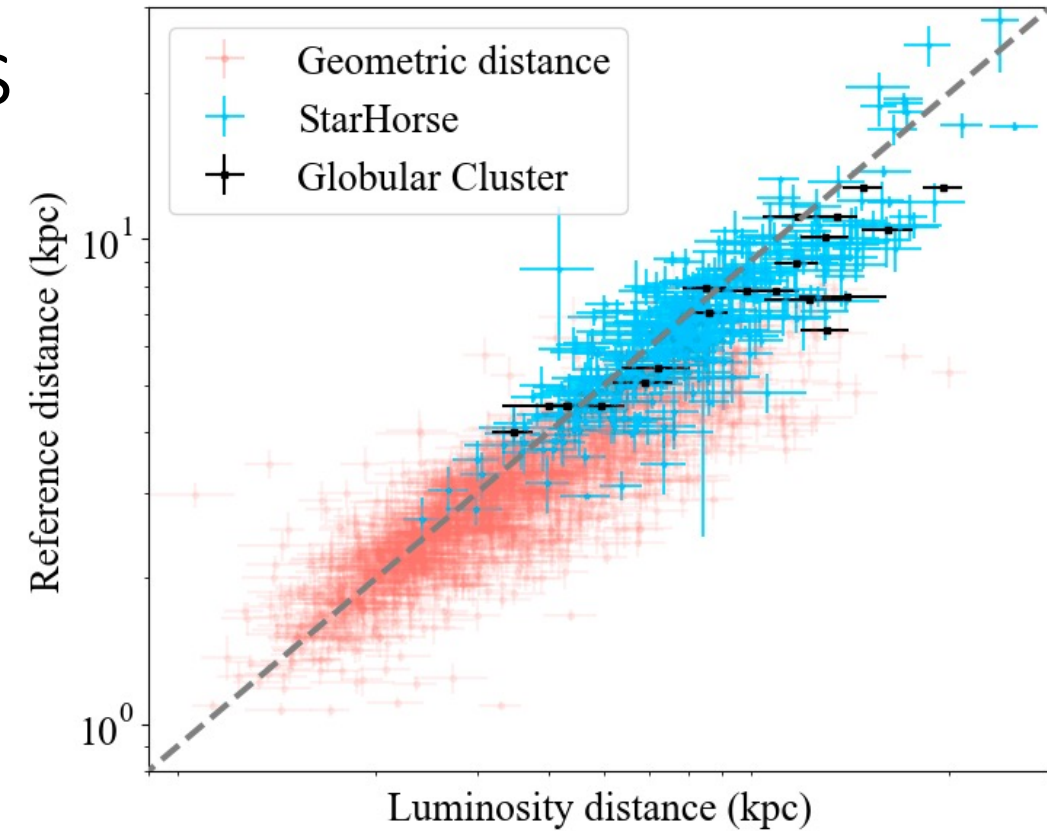
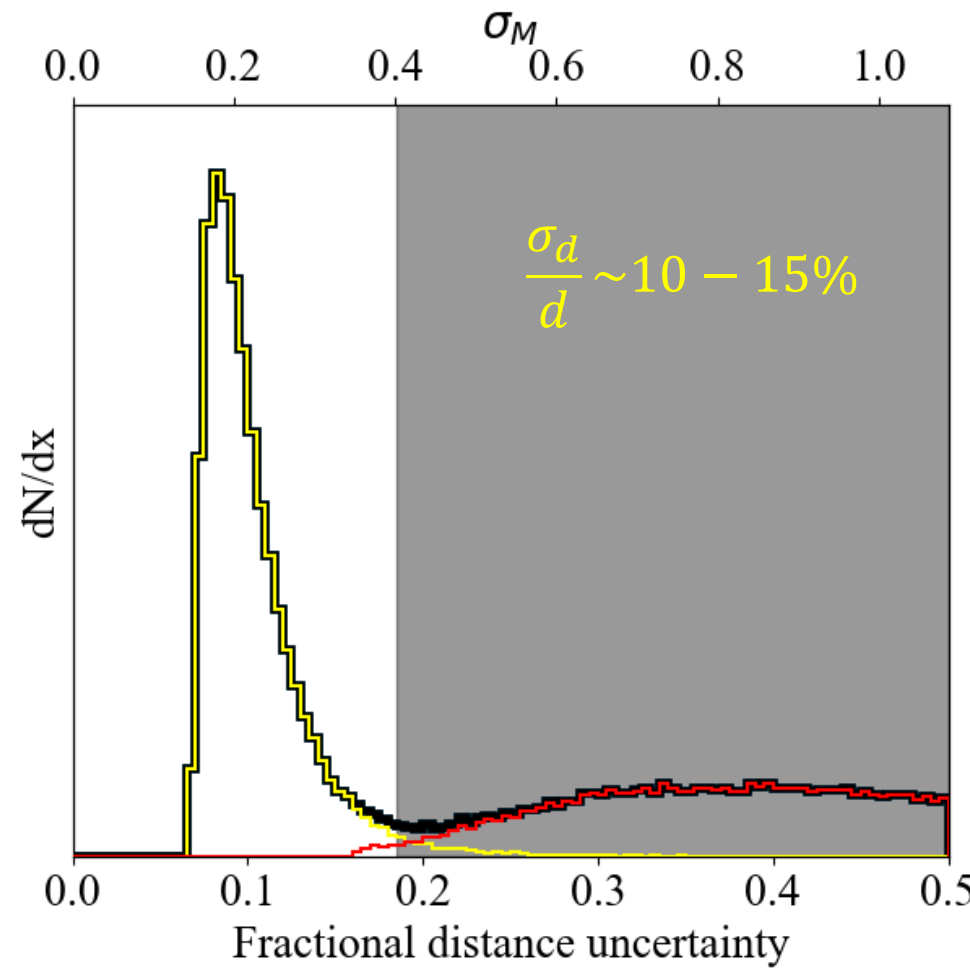


Period-Luminosity plane in Gaia LPV catalogue

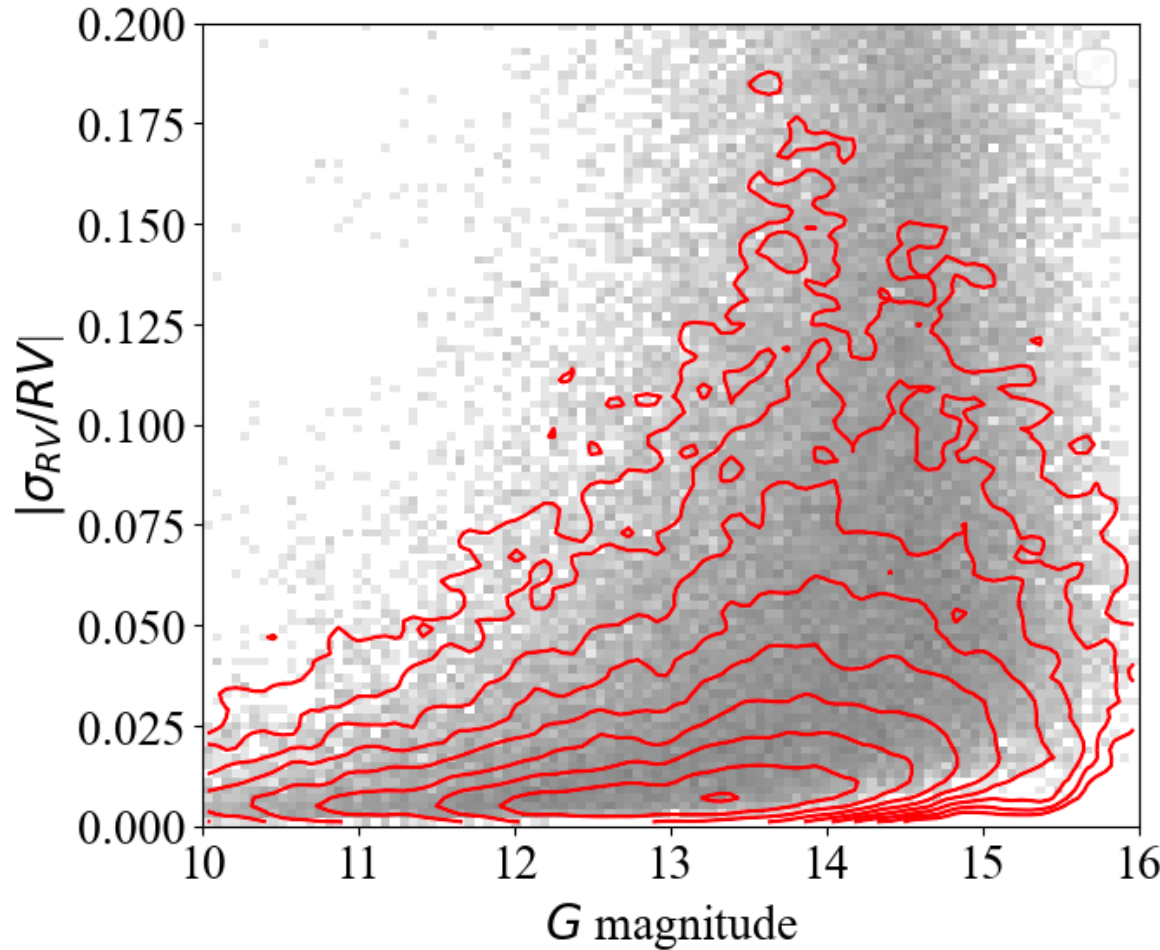
- Only one characteristic period can be extracted from the *Gaia* light curve
- Using the light curve amplitude to distinguish LA-LPV from SRV and Miras



Validation of luminosity distances



Is the line-of-sight velocity bad due to the variability? – NO

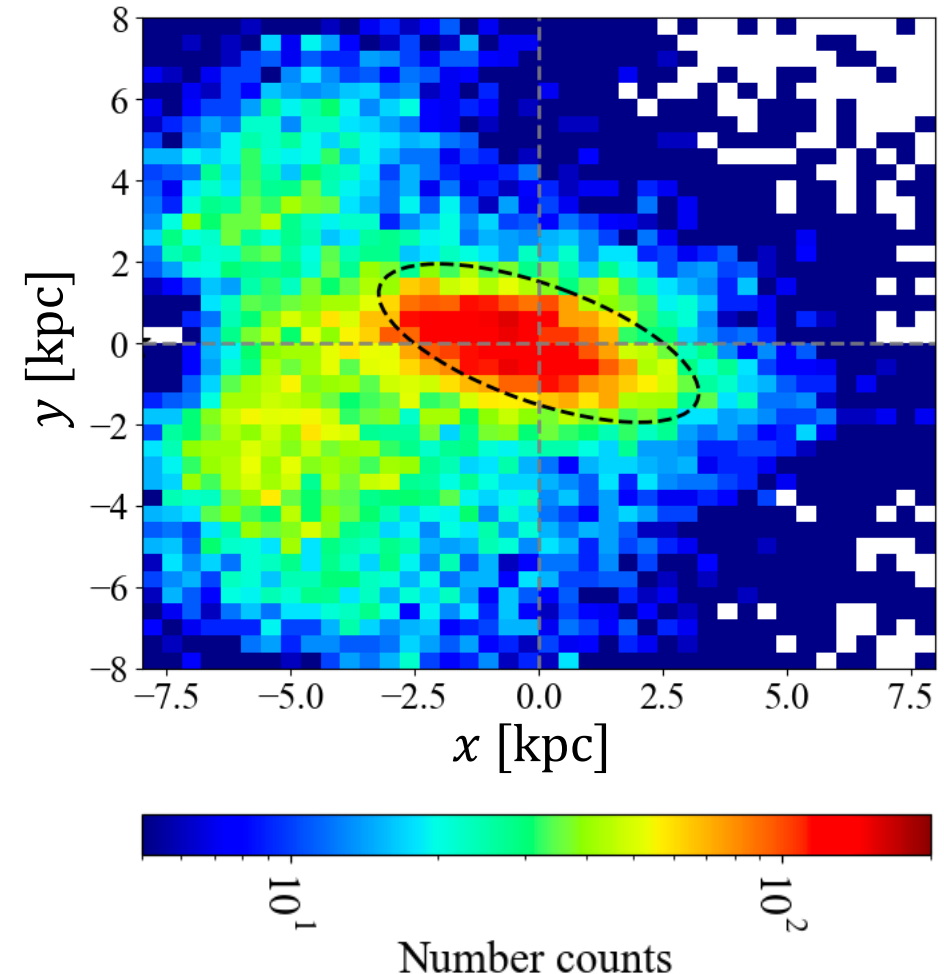


- Black 2D histogram in the background:
Randomly selected Gaia DR3 stars
- Red contour in the foreground:
LA-LPVs in this sample

The identical distribution in this plane verified the reliability of the Gaia line-of-sight velocity measurement for these LA-LPVs

Why the spatial selection function is minor

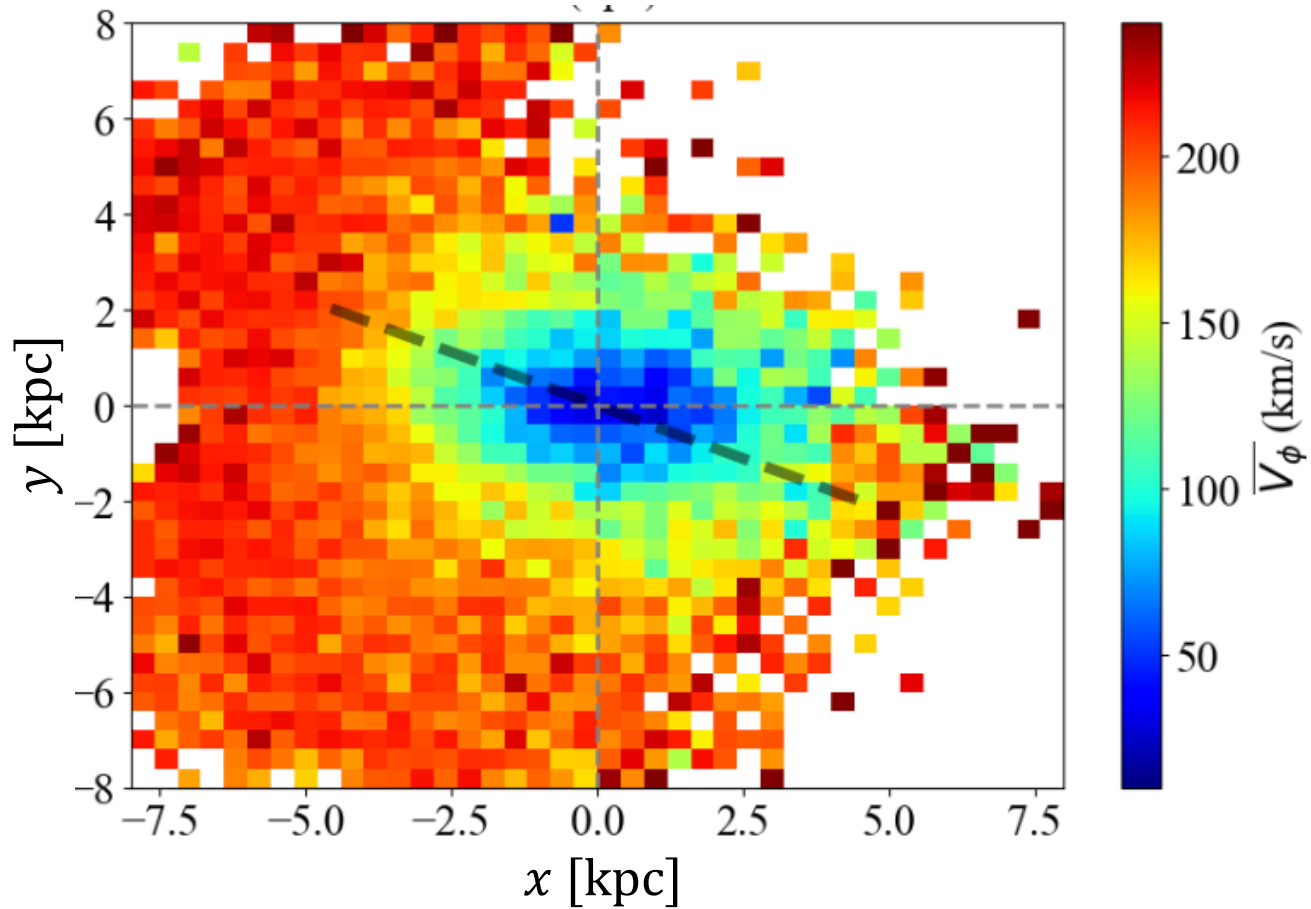
- Gaia full-sky coverage avoid sharp cutoff around the edge of footprints (unlike OGLE and APOGEE)
- Mostly photometric selections avoid strong selection function in magnitude
- The amplitude and period selections restrict the brightness of the star to $-7 < M_{JK} < -8$, which cancel out the magnitude selection function to the first order



Kinematics of the LA-LPV sample

Sanity check: Mean azimuthal velocity map

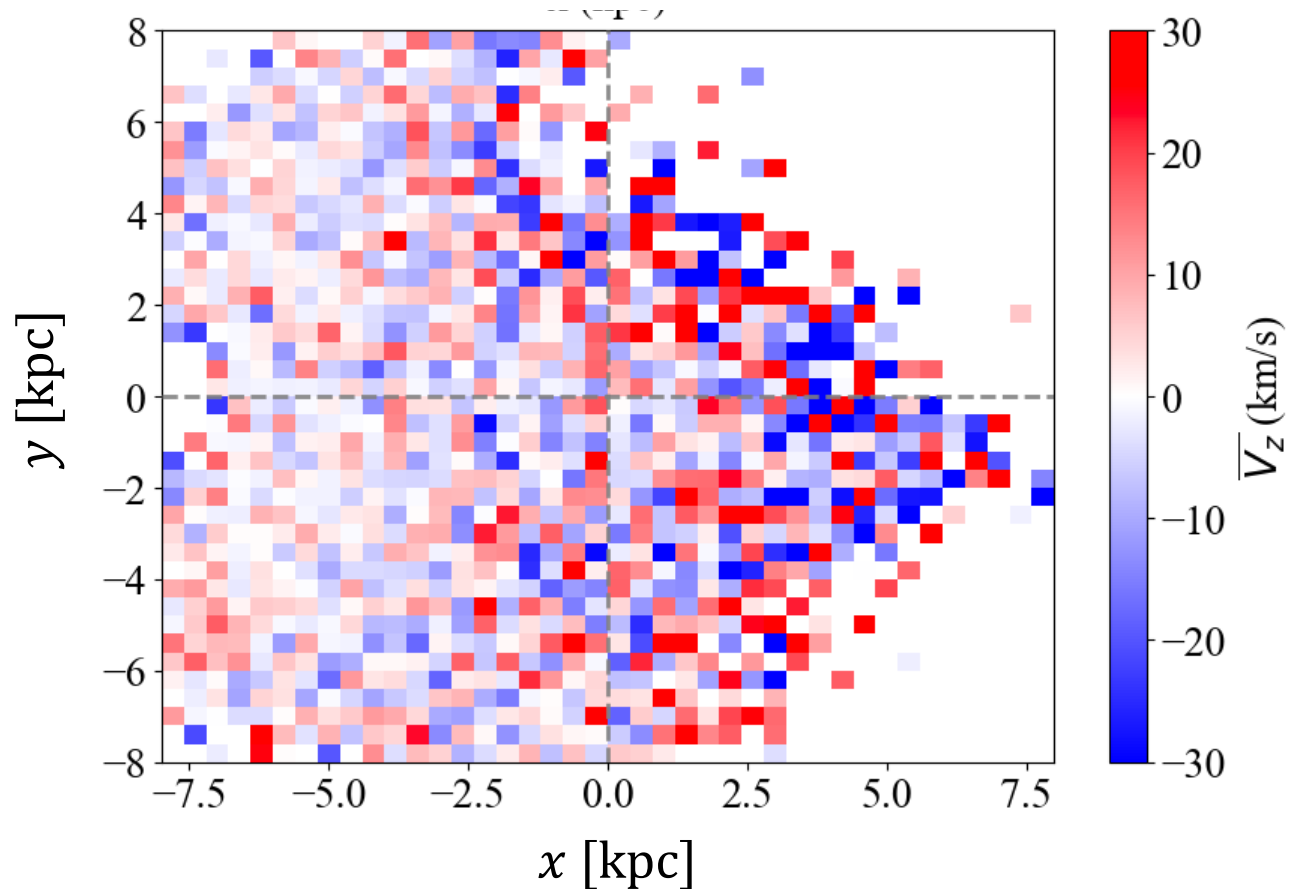
- Constant rotation curve at large radii (around the solar vicinity)
- Rotation drops to almost zero at the very inner centre (see Leung+23)



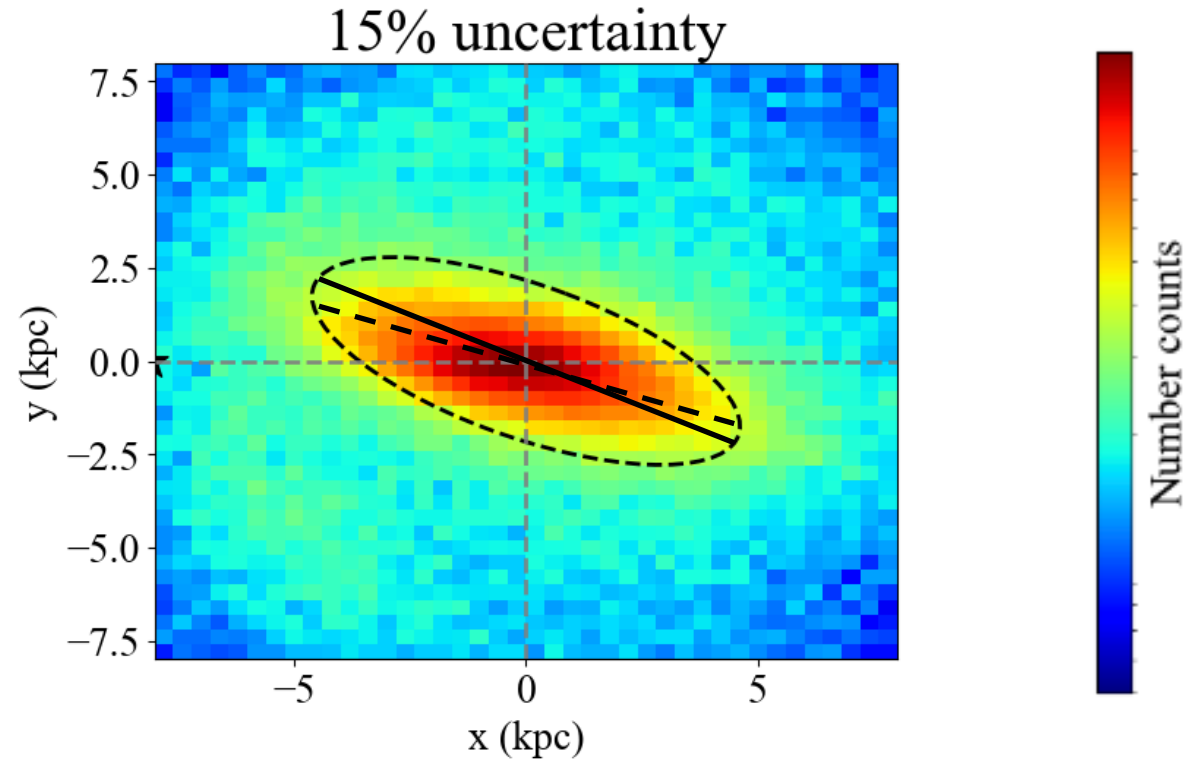
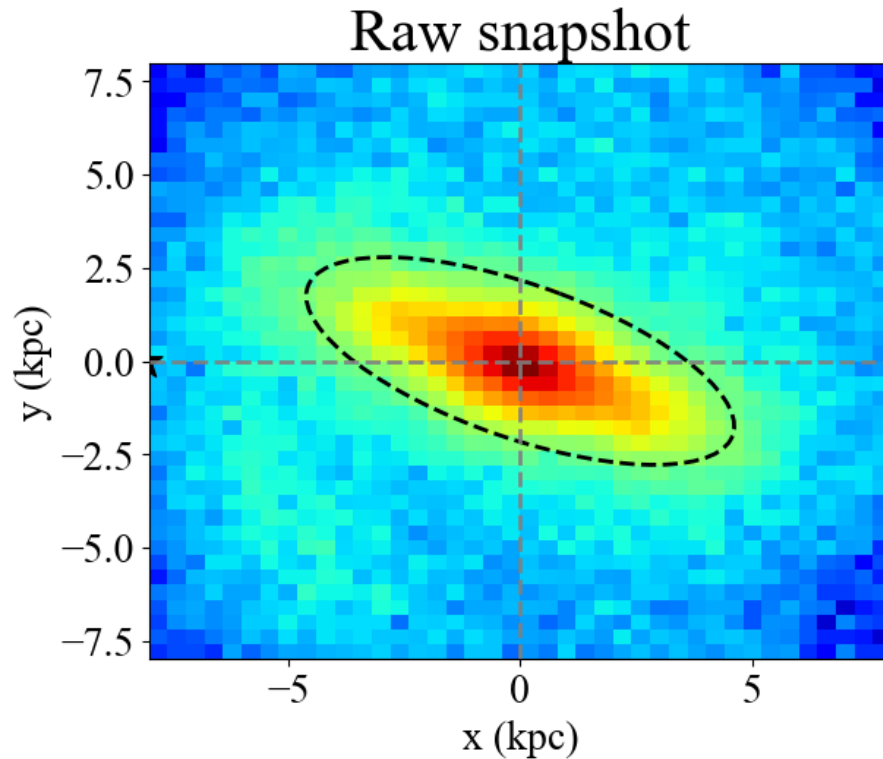
Kinematics of the LA-LPV sample

Mean v_z map

- No obvious signal is seen, which means the inner Galactic is vertically dynamically quiet

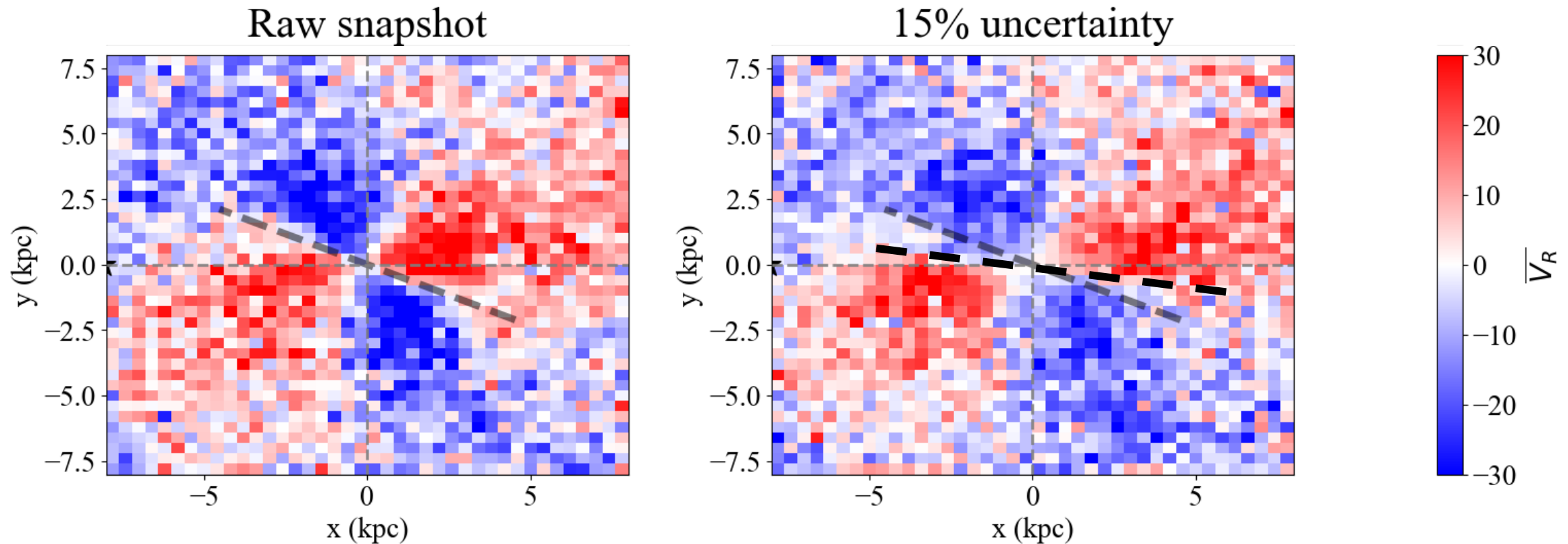


Effects of the heliocentric distance uncertainty



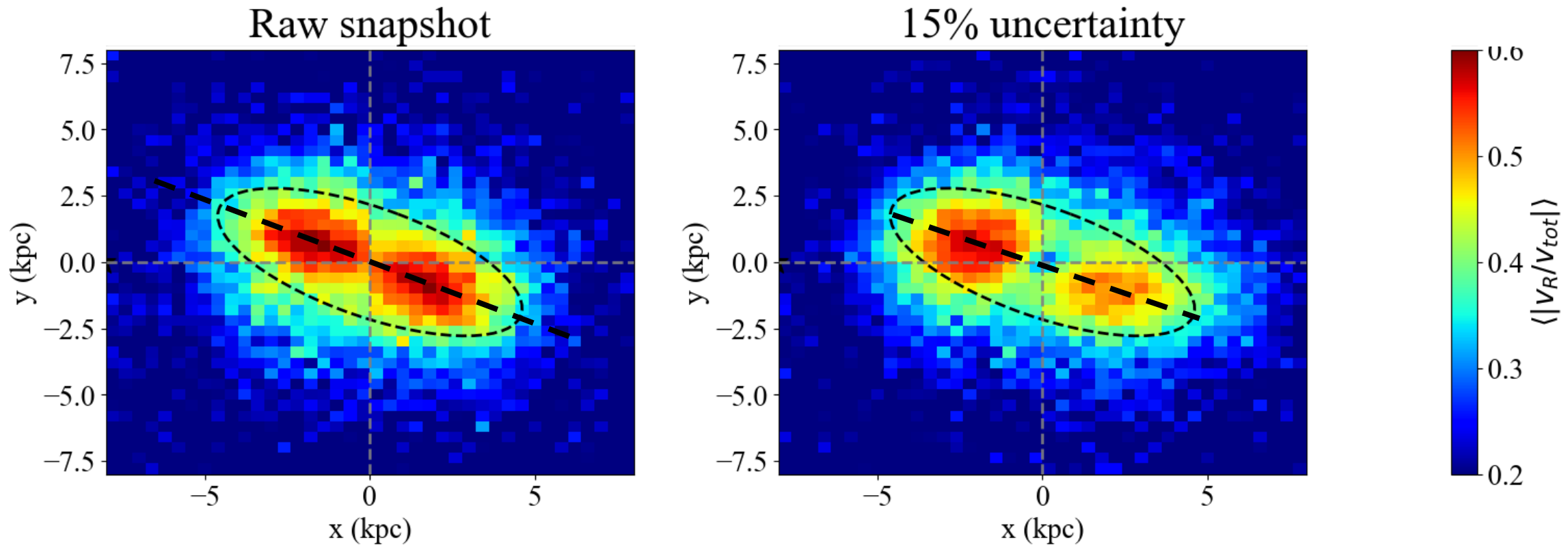
- Distance uncertainty smears each star along the line-of-sight direction bending the major-axis of the bar from its truth to the Sun-GC line

Effects of the heliocentric distance uncertainty



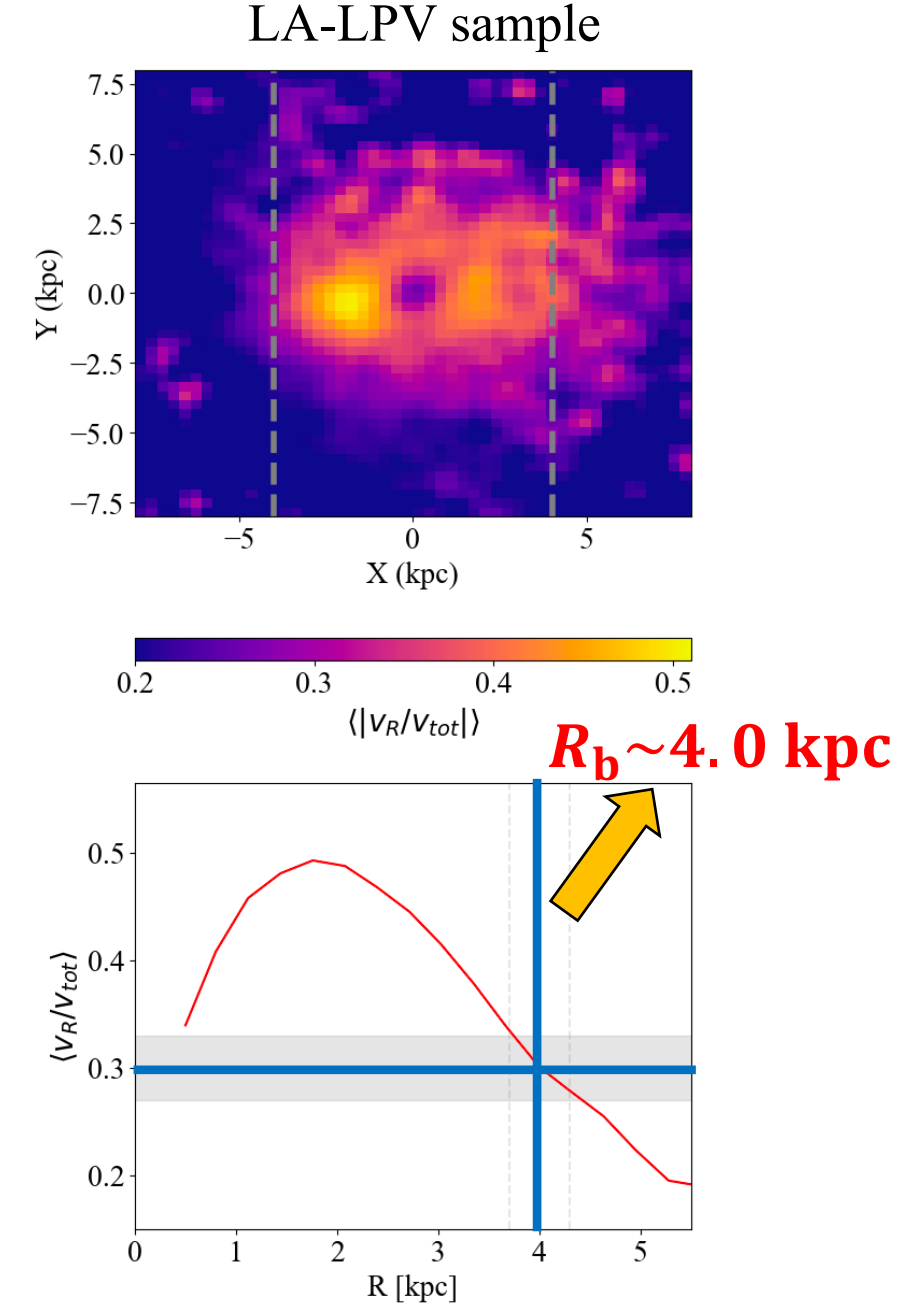
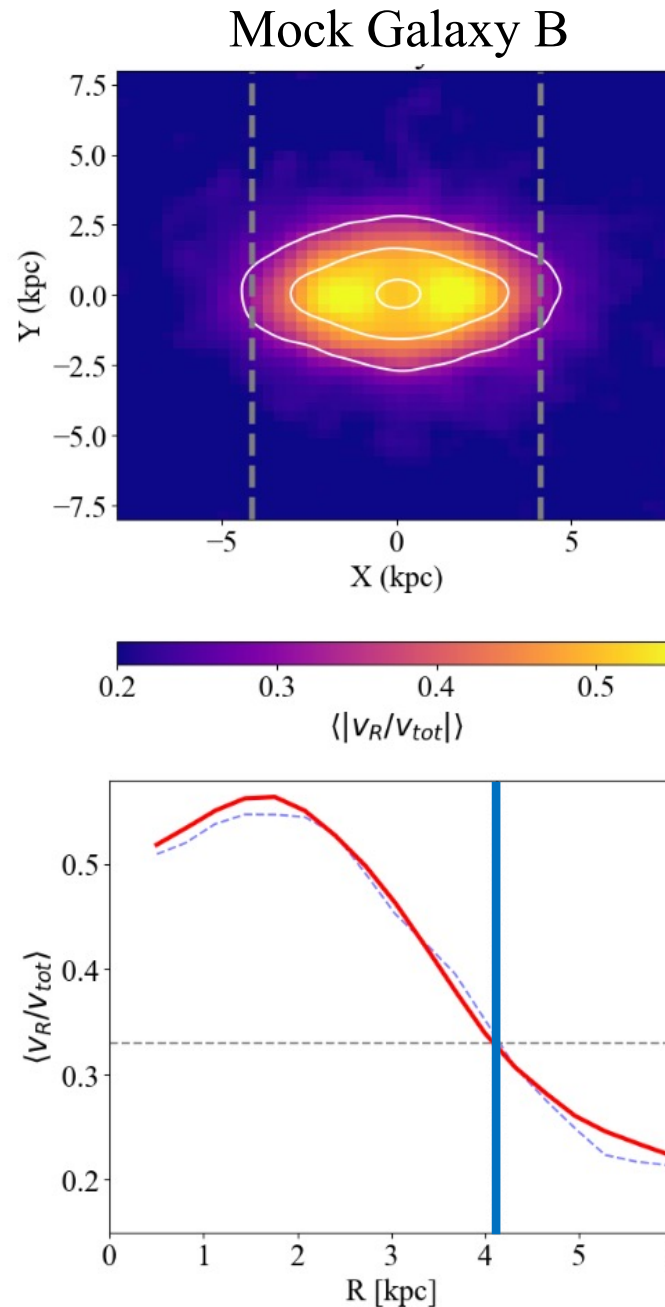
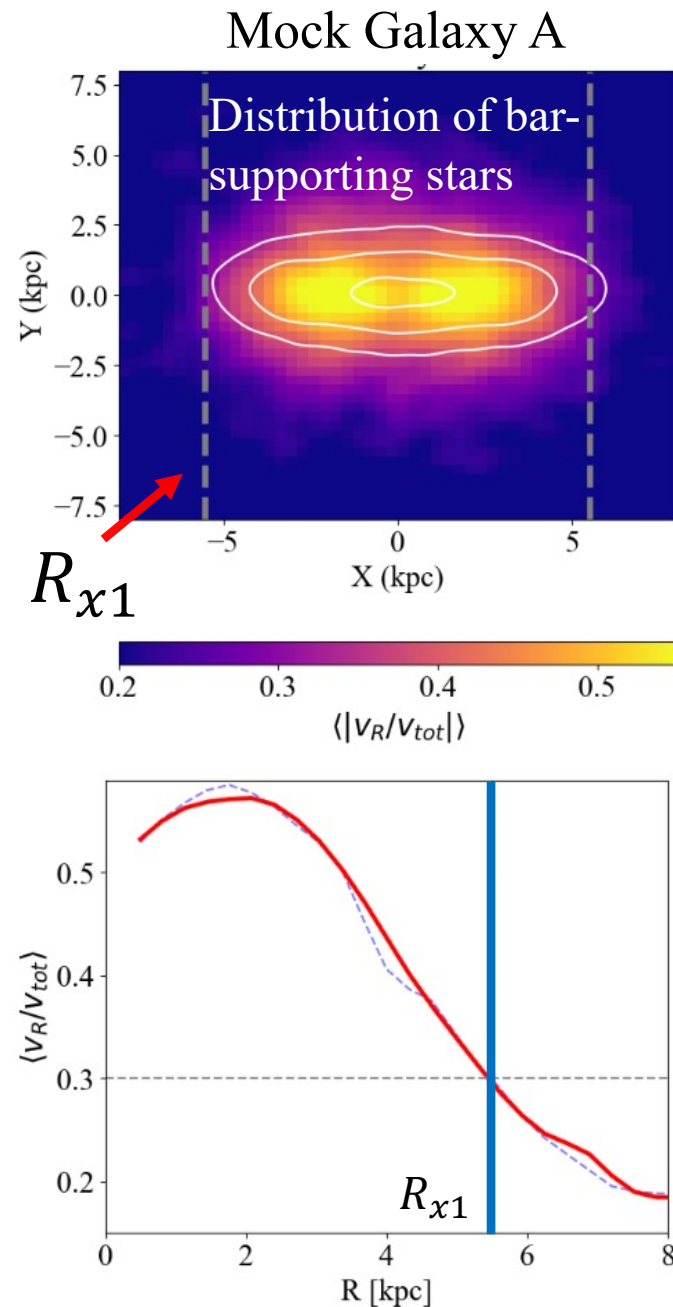
- The $\langle v_R \rangle$ map is even more biased, which demonstrates that the distance uncertainty in the Galactic bar region propagated in a non-Gaussian manner!

Effects of the heliocentric distance uncertainty

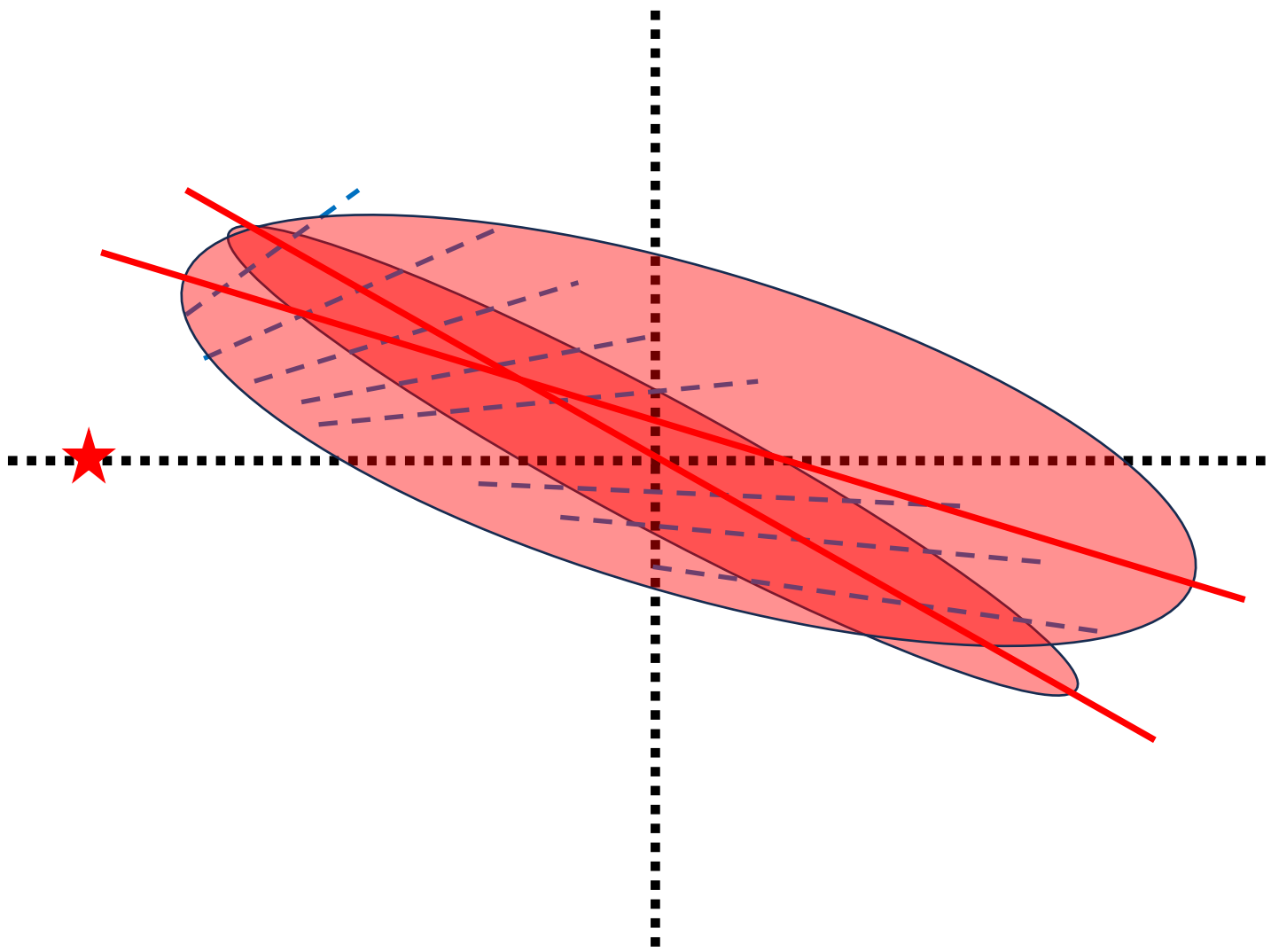


- The $\langle |v_R|/v_{tot} \rangle$ maps are much less affected by the distance uncertainty comparing to the $\langle v_R \rangle$ map because it is dimensionless

Kinematically estimate the dynamical length of the bar



Bias due to the distance uncertainty



Estimation of the pattern speed

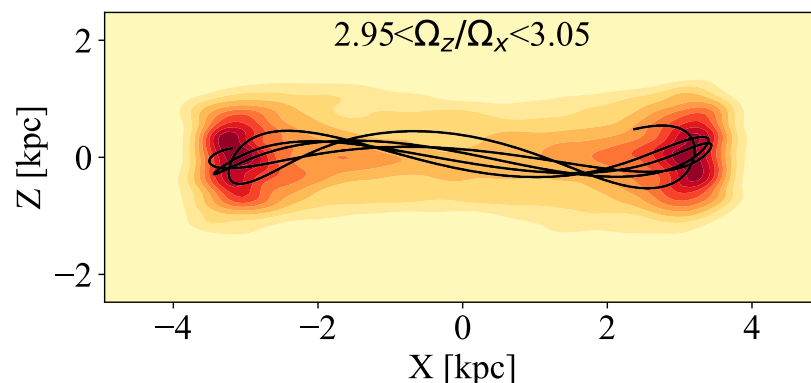
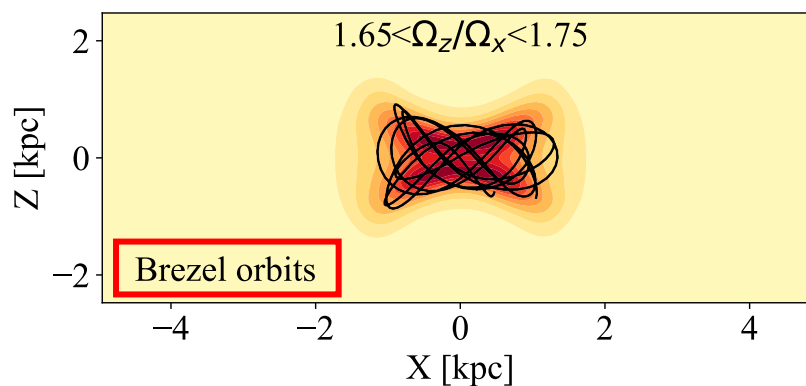
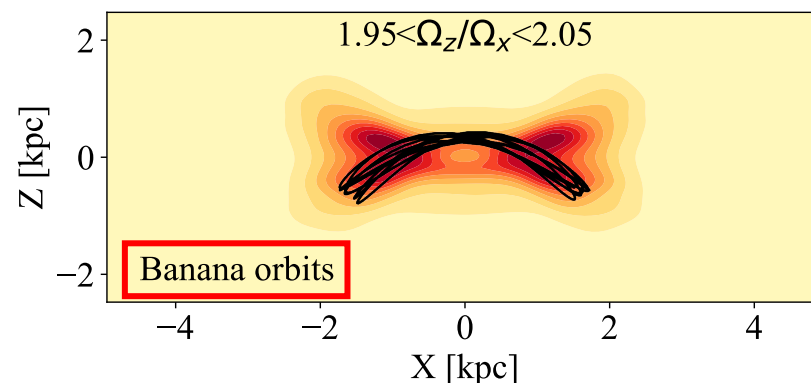
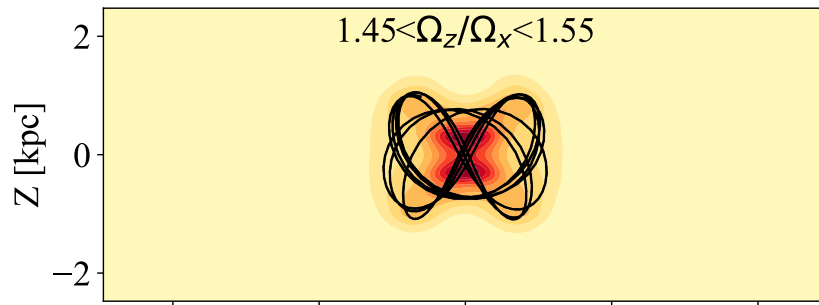
- Dehnen+23 developed a method to extract pattern speed from simulations using the continuity equation

$$\partial \rho / \partial t + \nabla \cdot (\rho \bar{\mathbf{v}}) = 0, \rightarrow \Omega = \frac{\int d^3x \boxed{\rho} [W \bar{\phi} + \frac{i}{m} \bar{v}_R (\partial W / \partial R)] e^{-im\varphi}}{\int d^3x \rho \boxed{W} e^{-im\varphi}}.$$

- Can't directly apply to any observation because:
 - The continuity equation can't handle uncertainties
 - This formulation also can't accept the azimuthal selection function
- We can test how much these two observational caveats would influence the pattern speed calculation using the N-body simulation snapshots

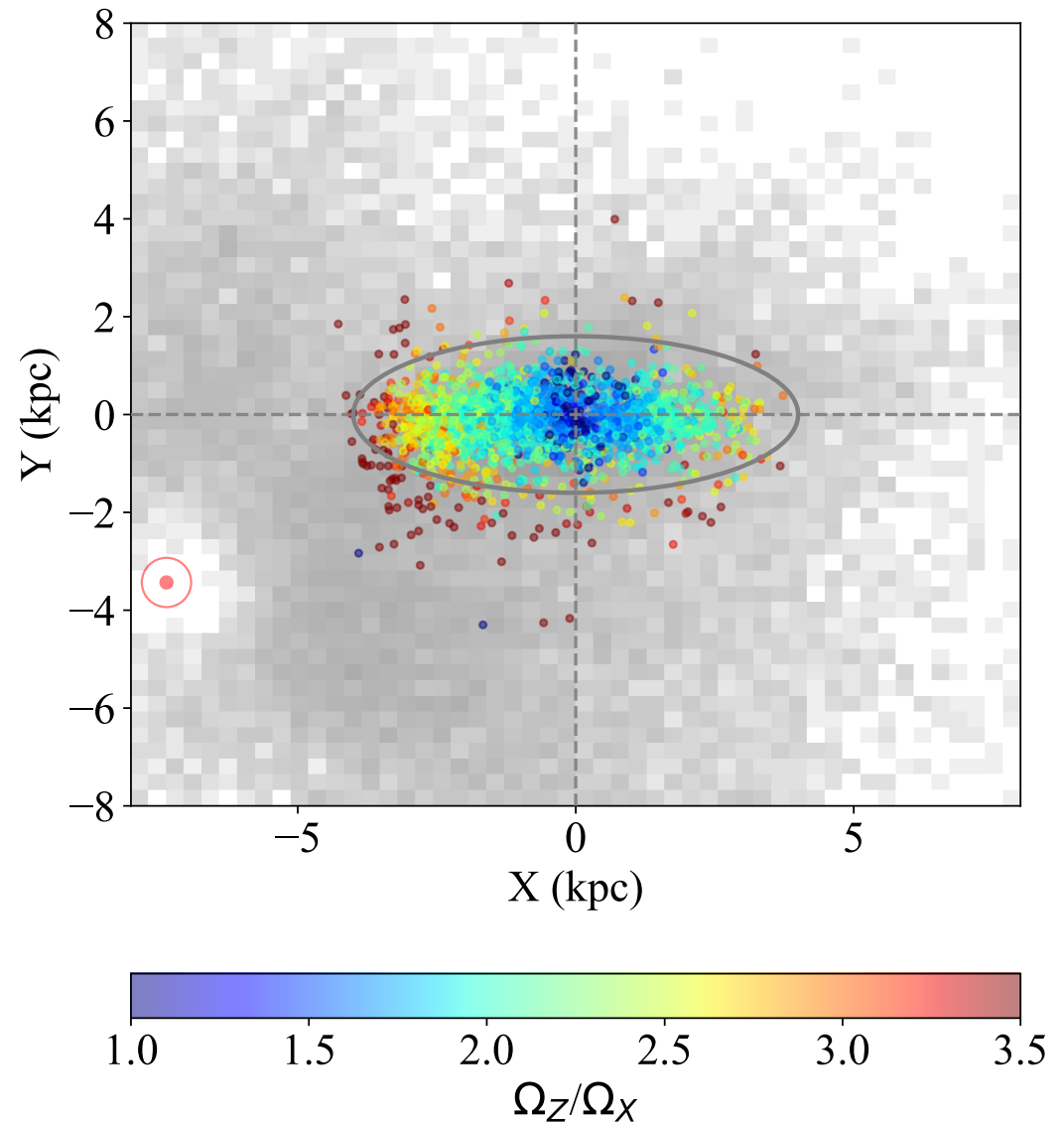
Play more with the dynamics!

- Assume the Galactic potential from the M2M model in Portail+17 (Sormani+22) is correct
- Select bar stars with $1.8 < \Omega_R/\Omega_X < 2.2$
- Shed light on the vertical structure of the bar using the Ω_Z/Ω_X value



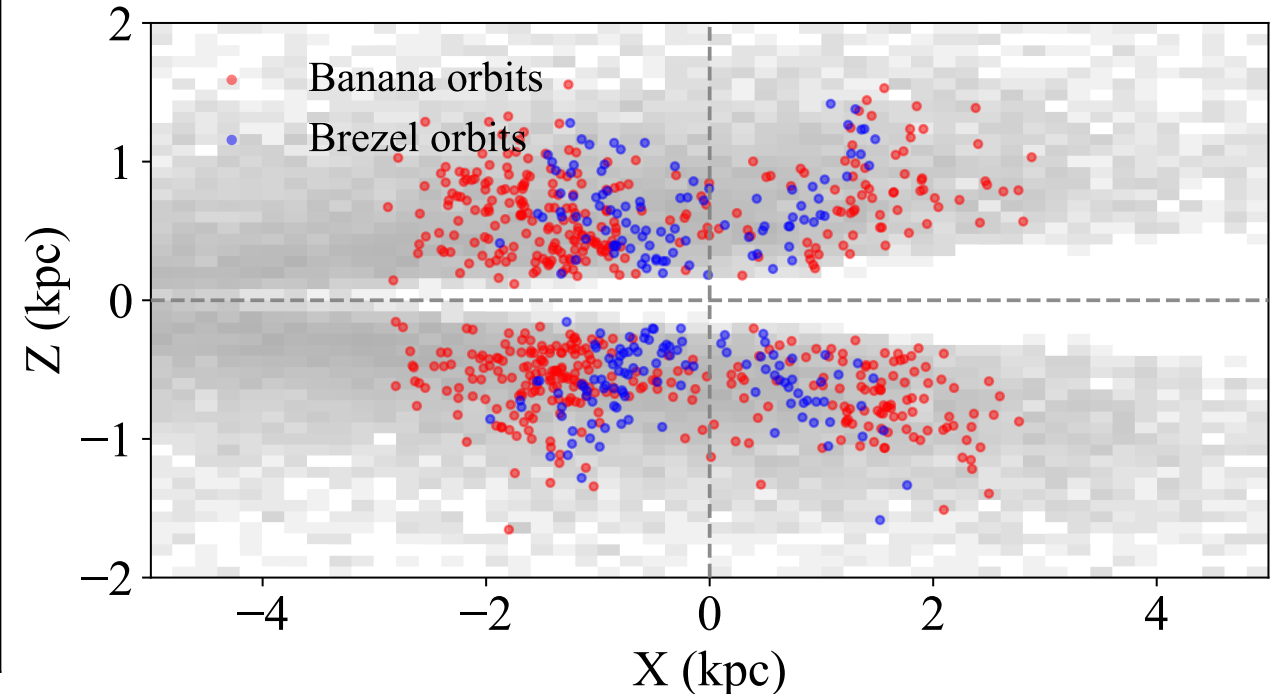
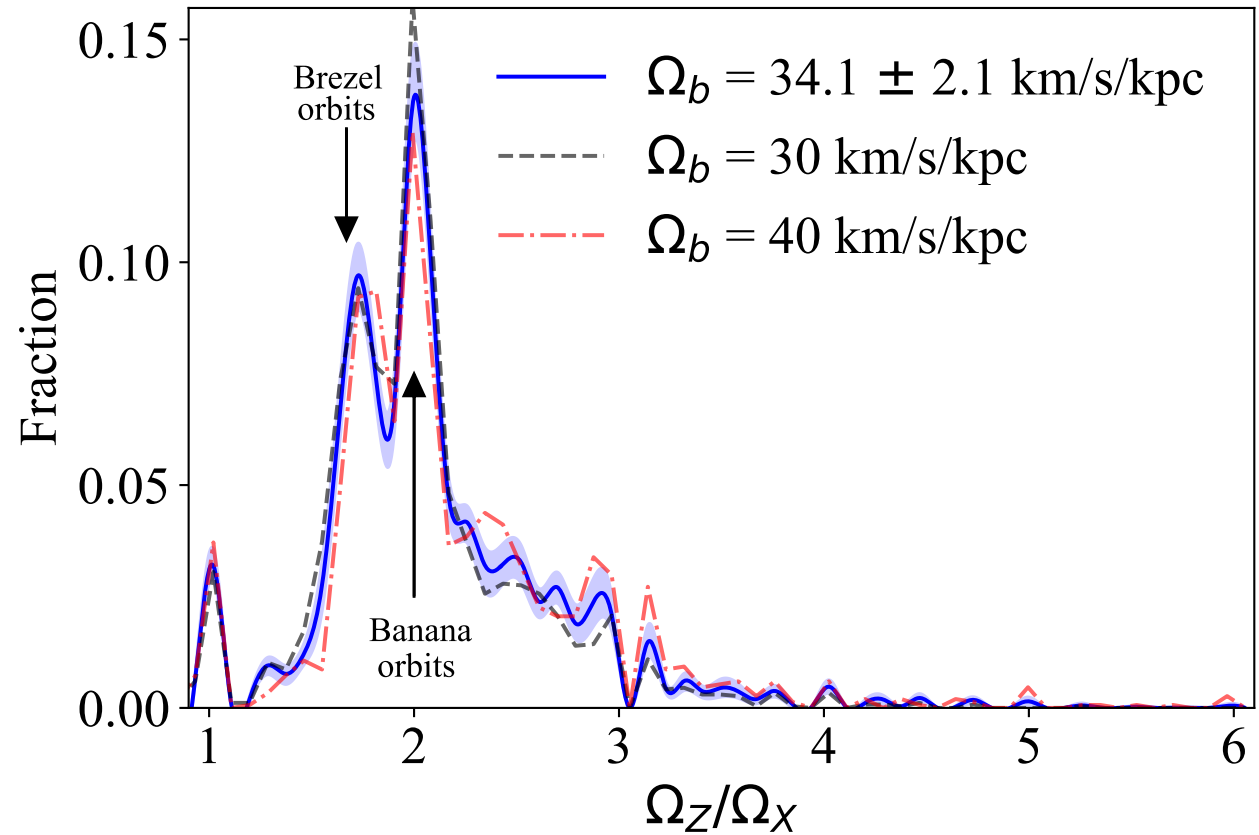
In-plane distribution of bar stars

- Stars with greater Ω_z/Ω_x value span **larger** radius and reside **farther** from the Galactic centre

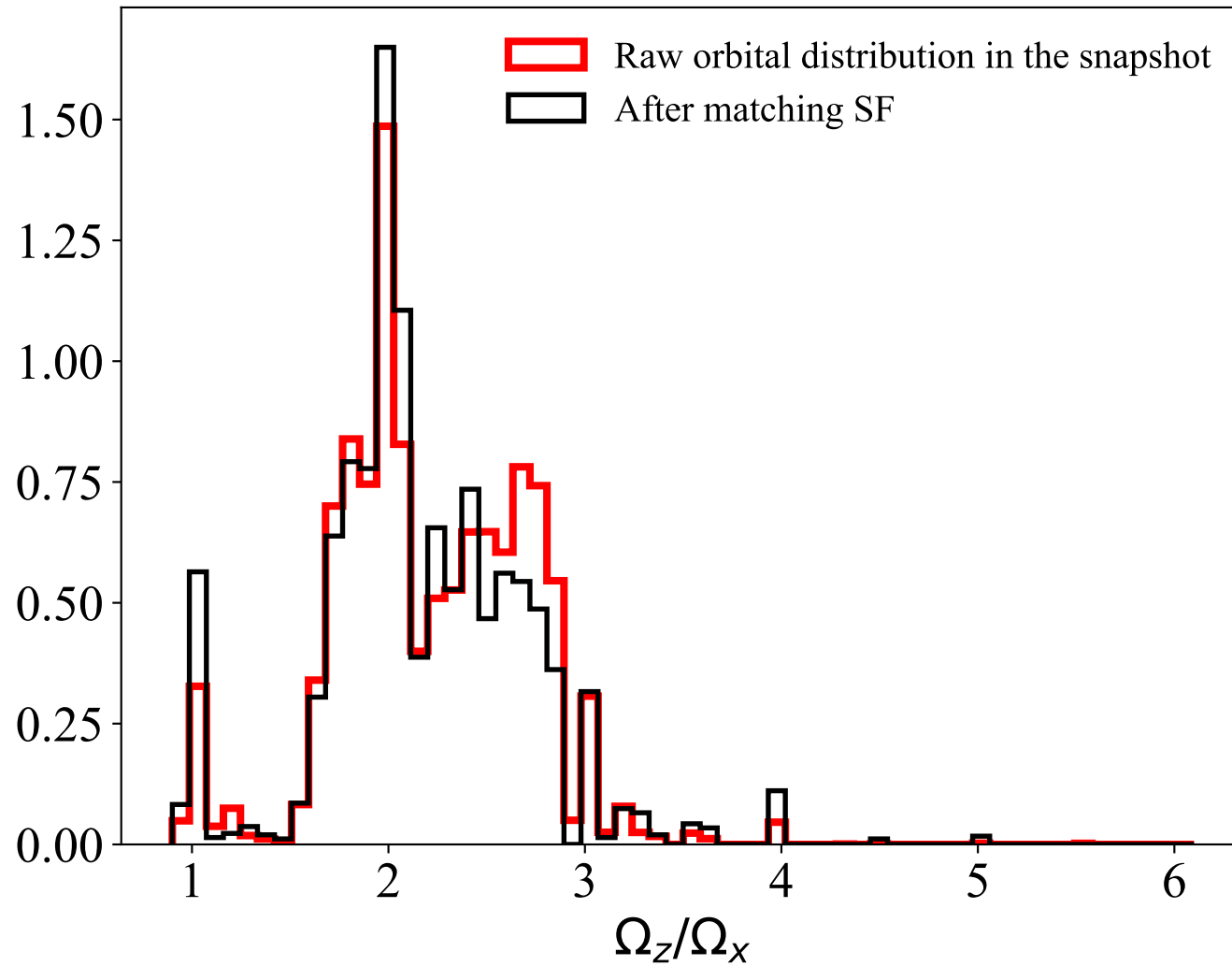


What contribute the Galactic X-shaped structure

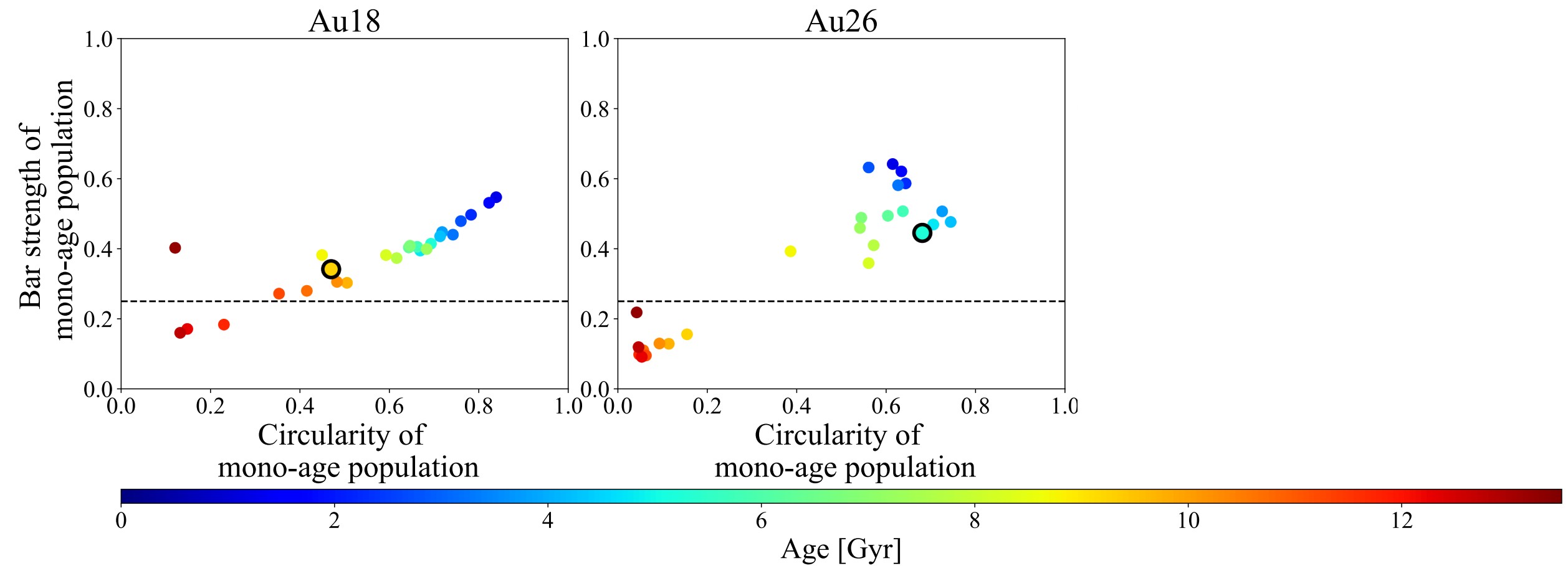
Banana or Brezel ?



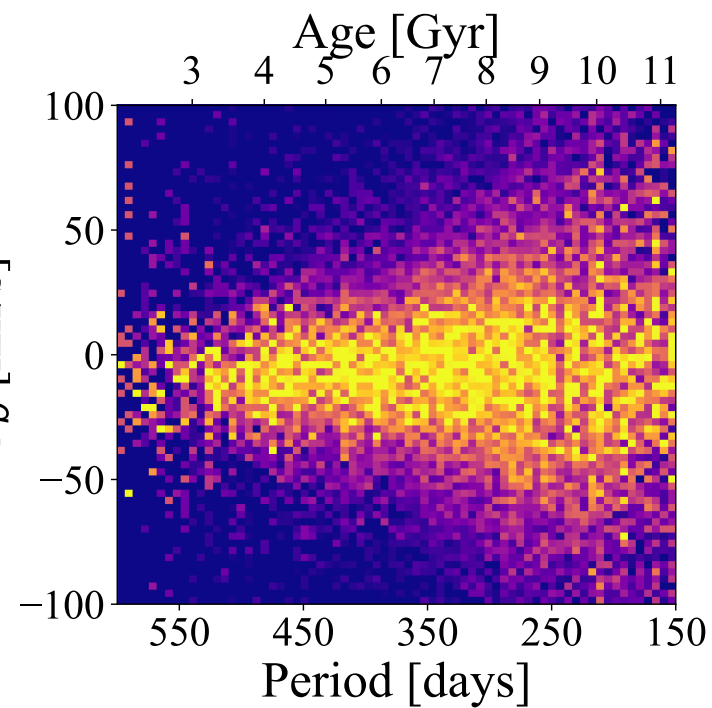
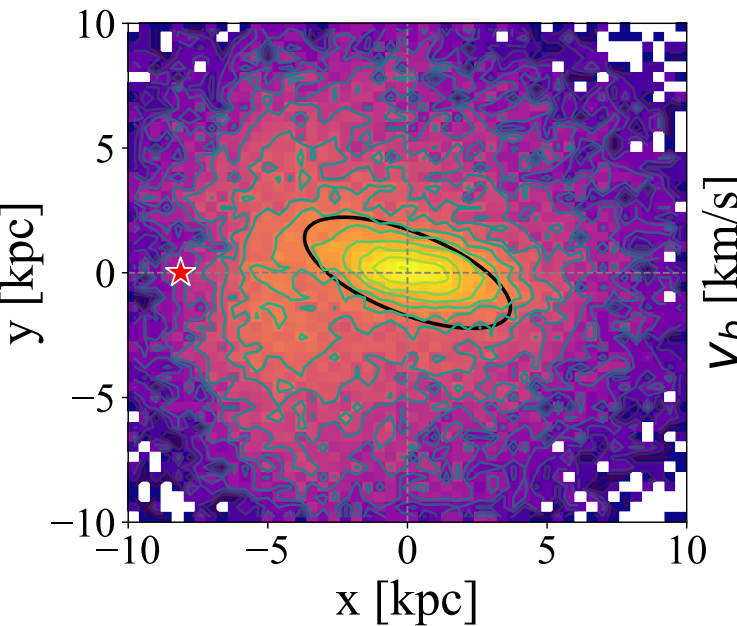
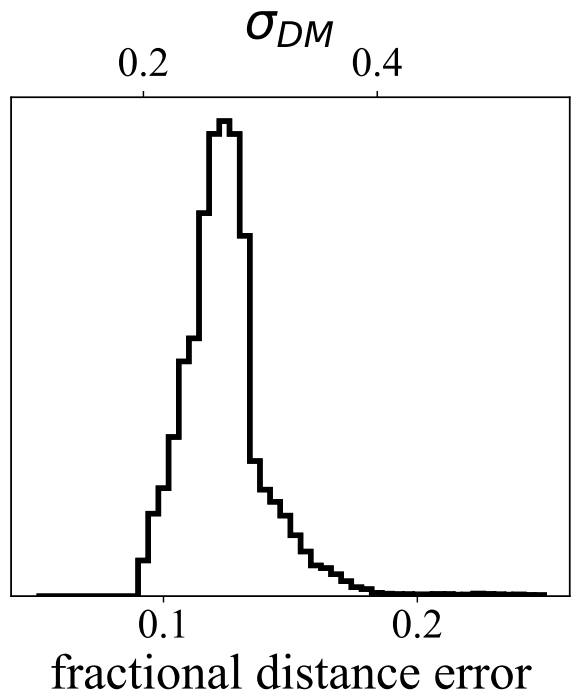
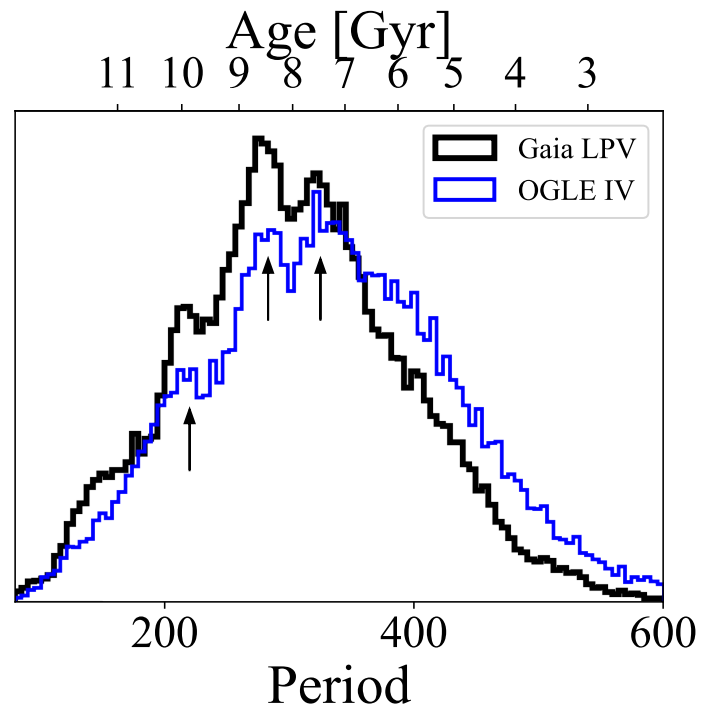
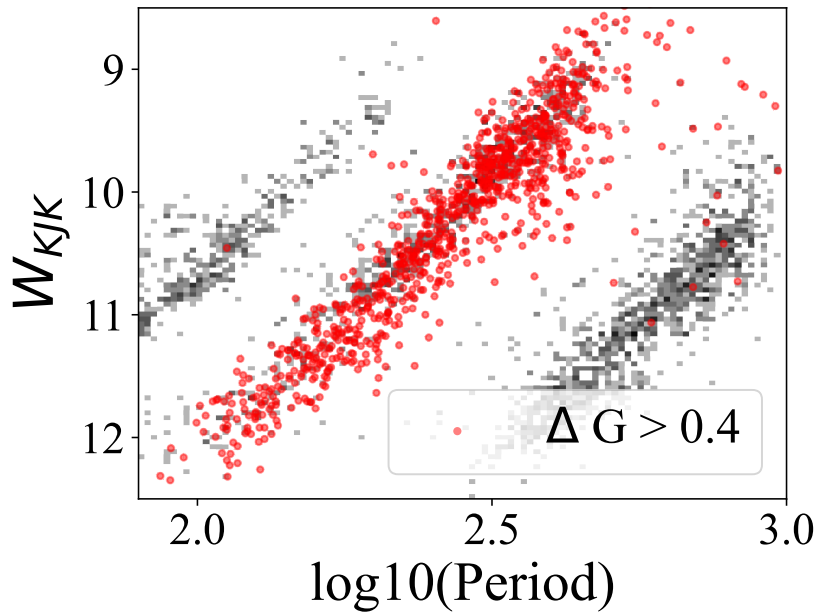
Selection function effect on bar orbital family distribution



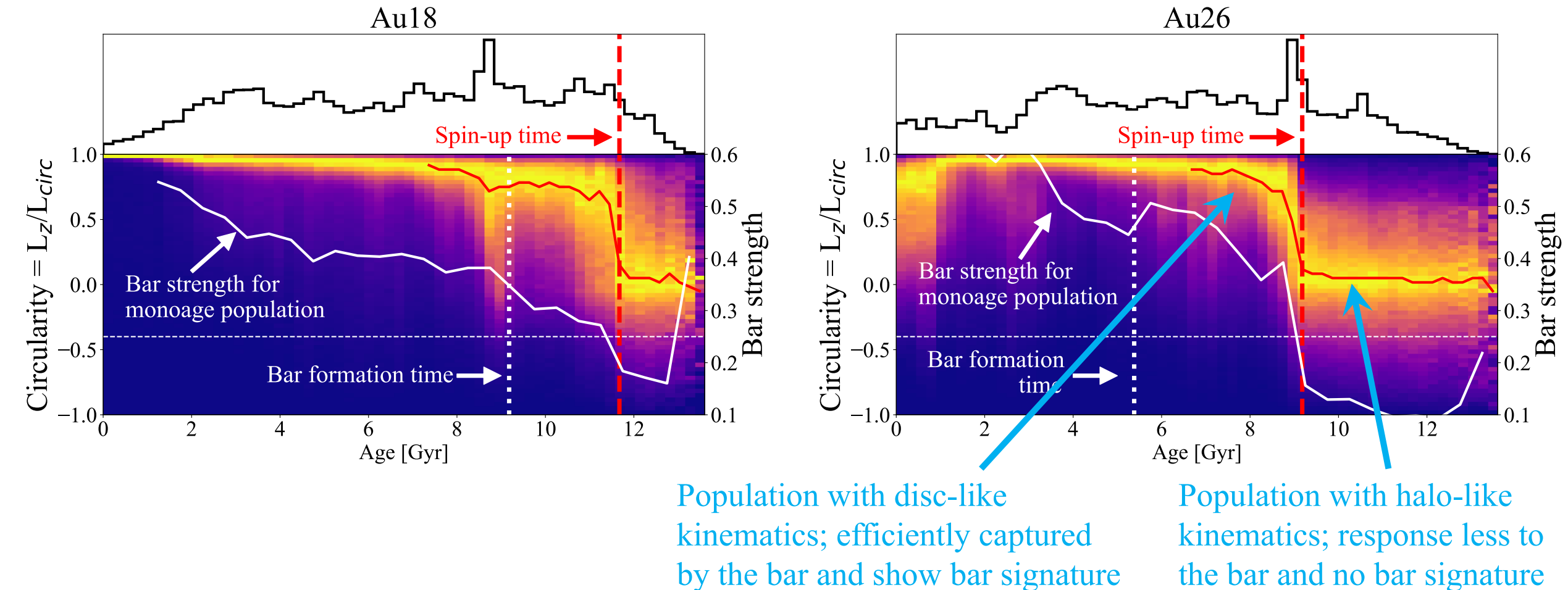
Correlation between kinematics and bar strength



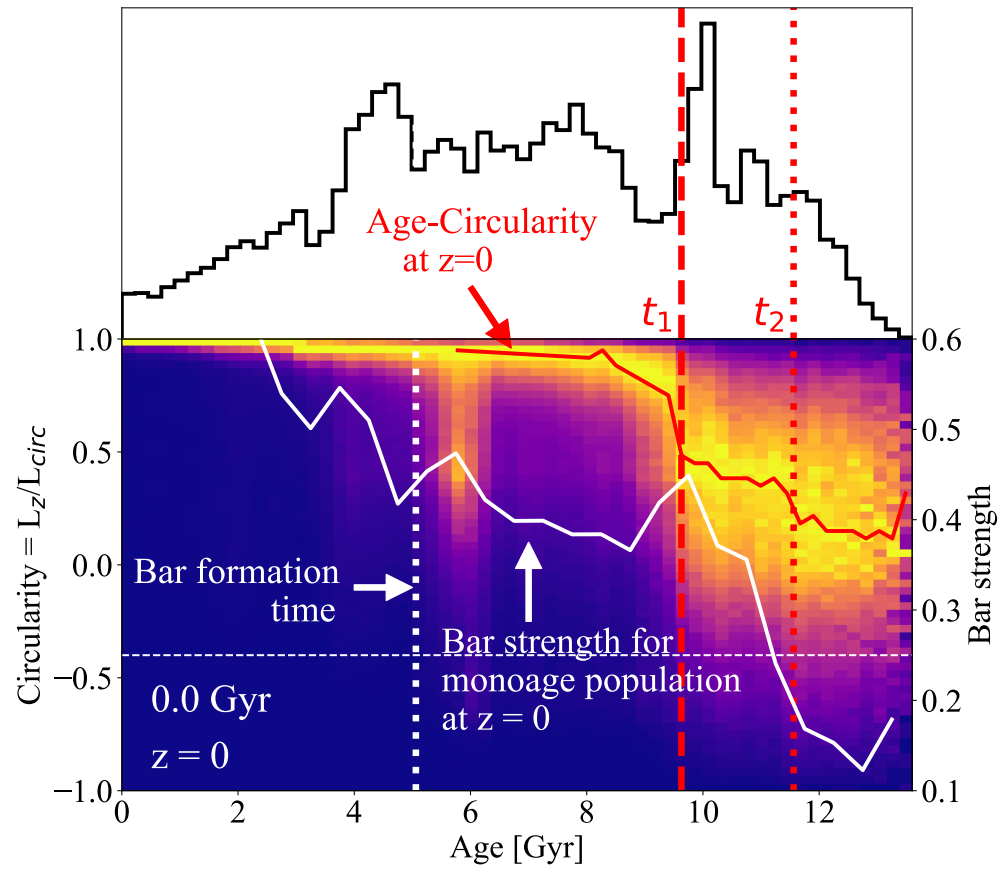
Mira sample property



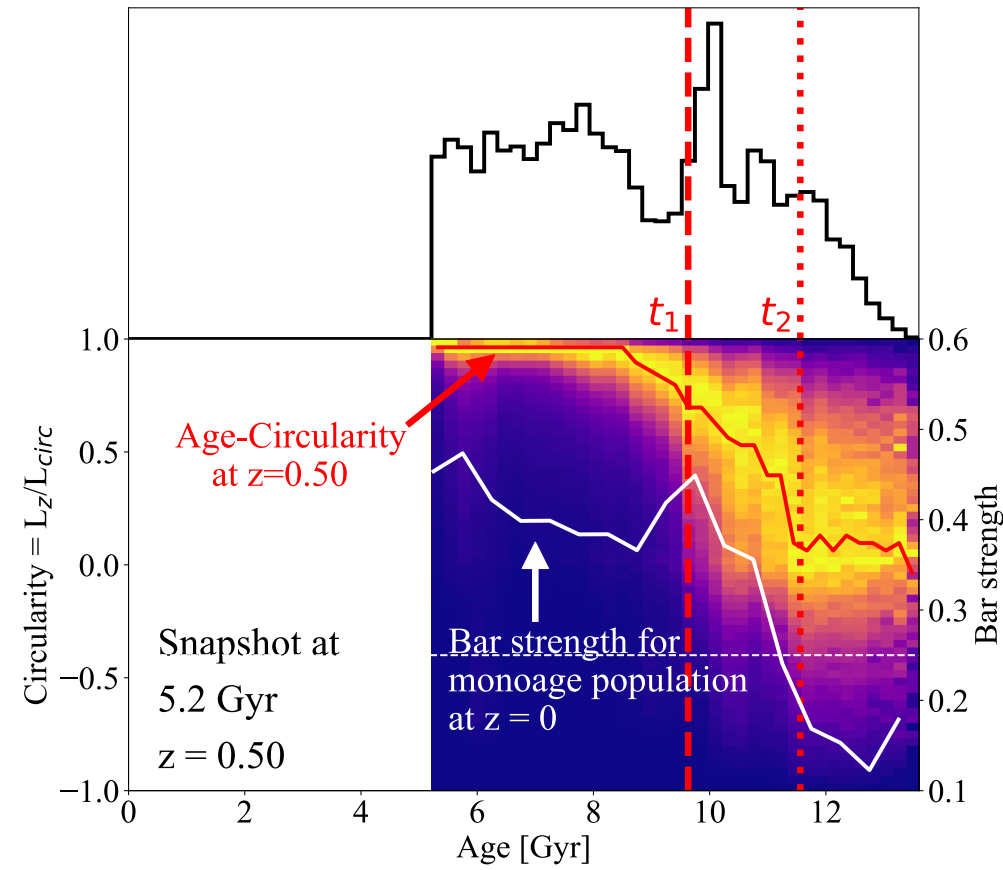
Auriga cosmological simulations: Spin-up in Au18 & Au26

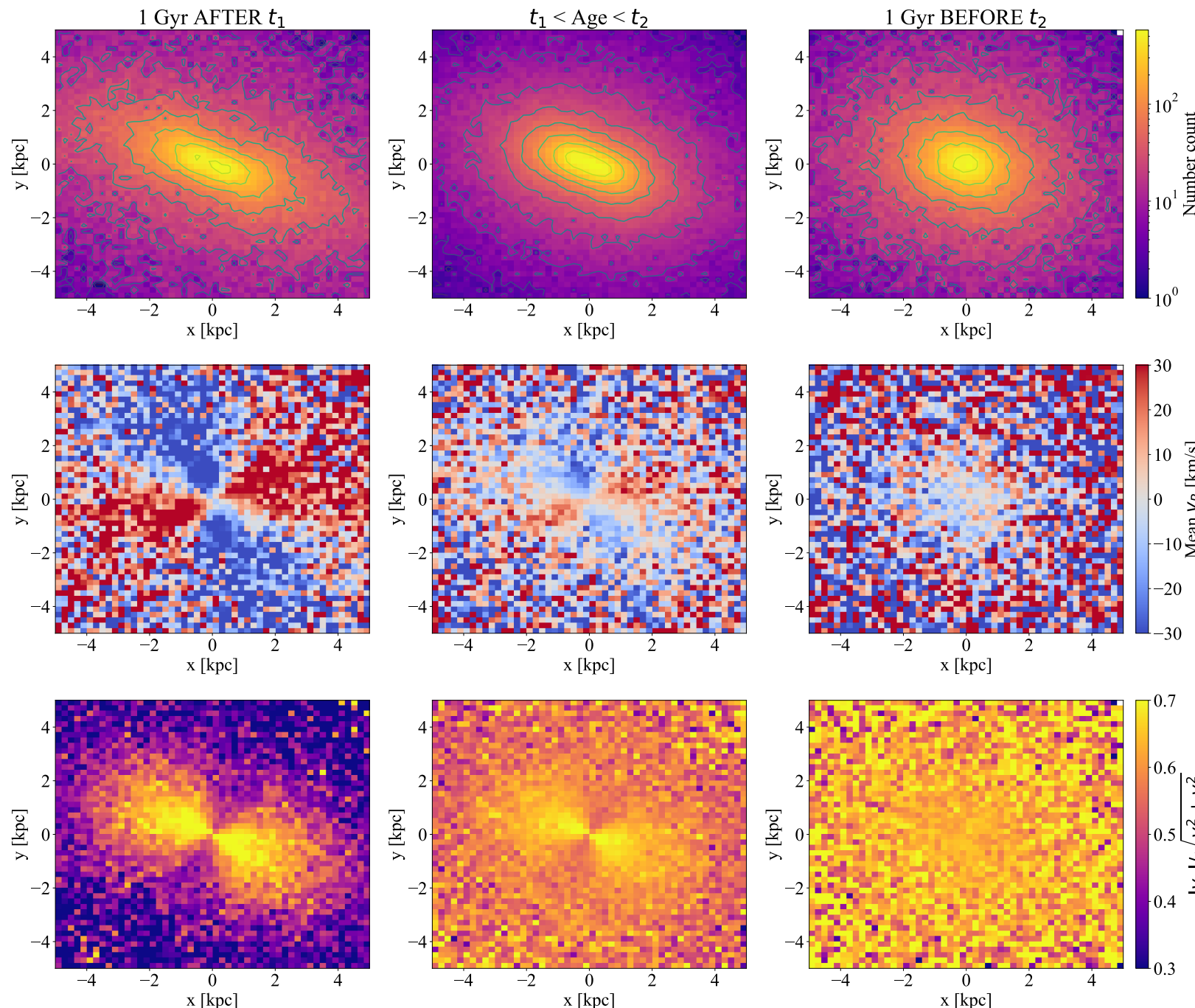


Au23



Au23

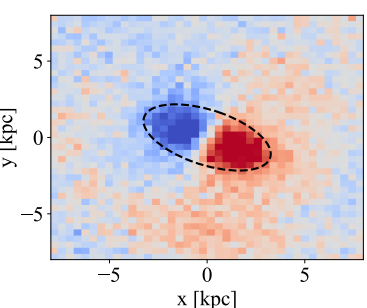
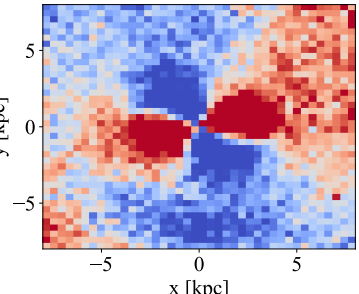




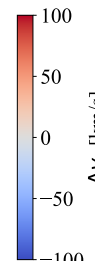
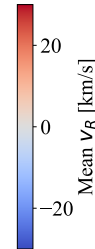
Use v_l map to track the chrono-kinematics of inner Galaxy: Au18 as an example

After the spin-up

$1 < \text{Age [Gyr]} < 3$



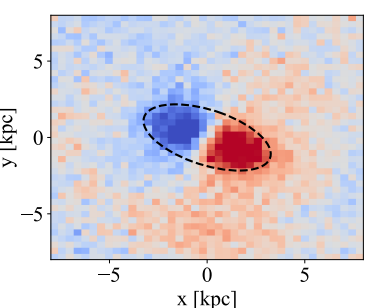
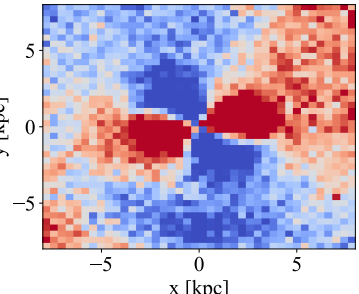
Before the spin-up



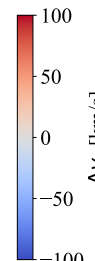
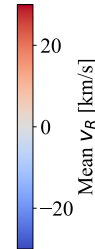
Use v_l map to track the chrono-kinematics of inner Galaxy: Au18 as an example

After the spin-up

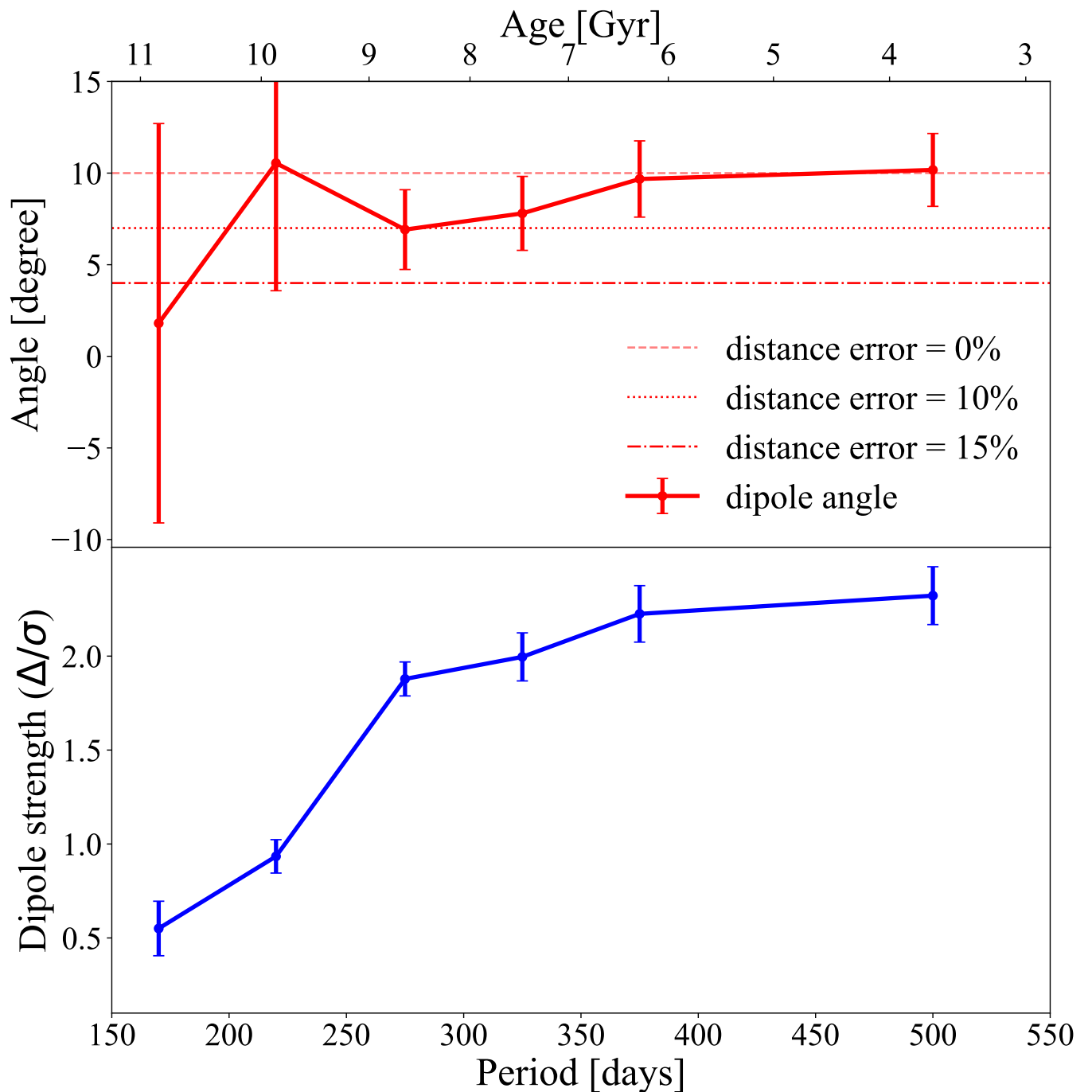
$1 < \text{Age [Gyr]} < 3$



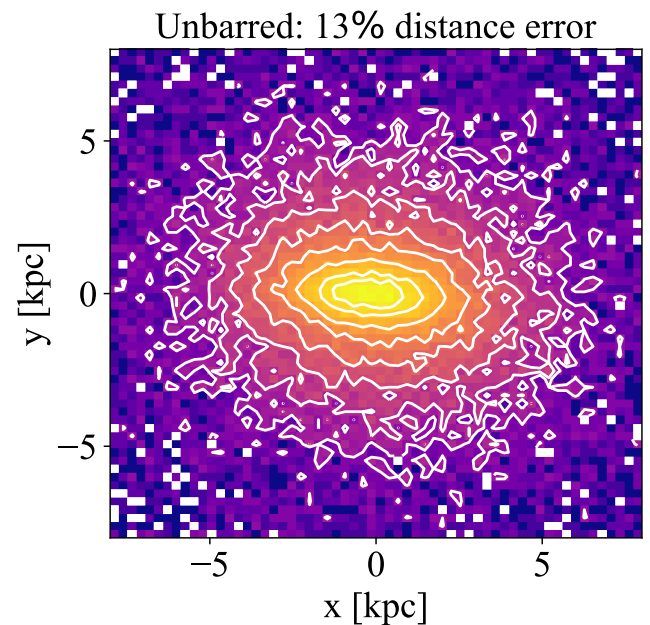
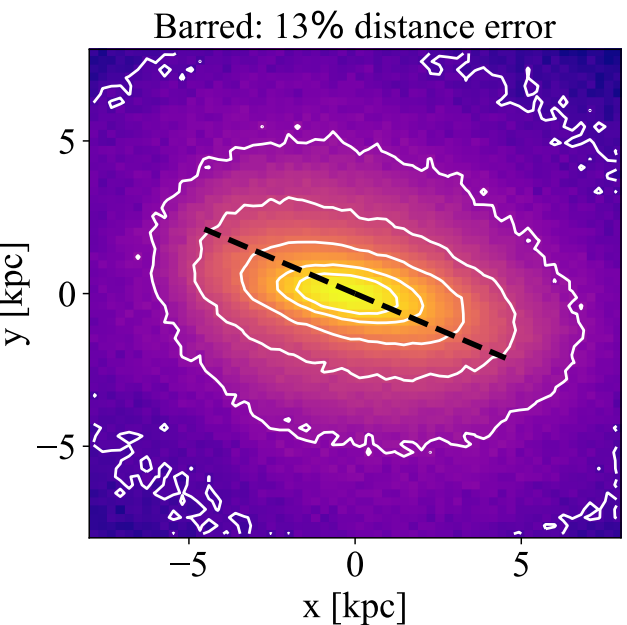
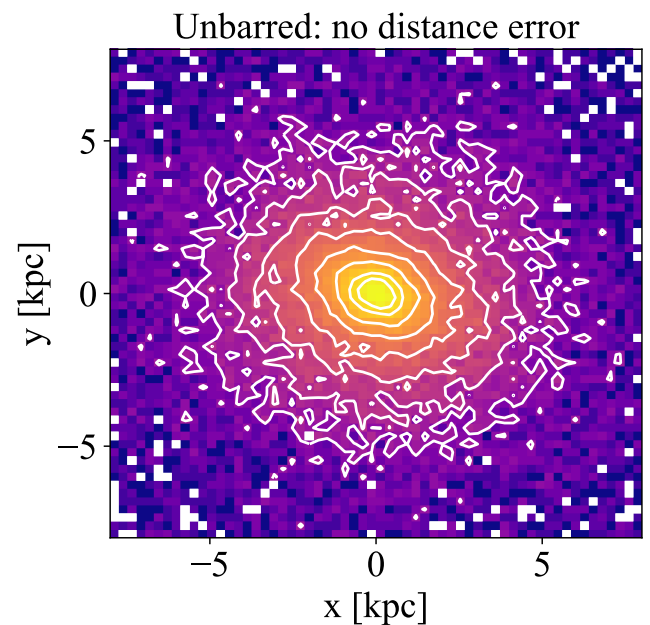
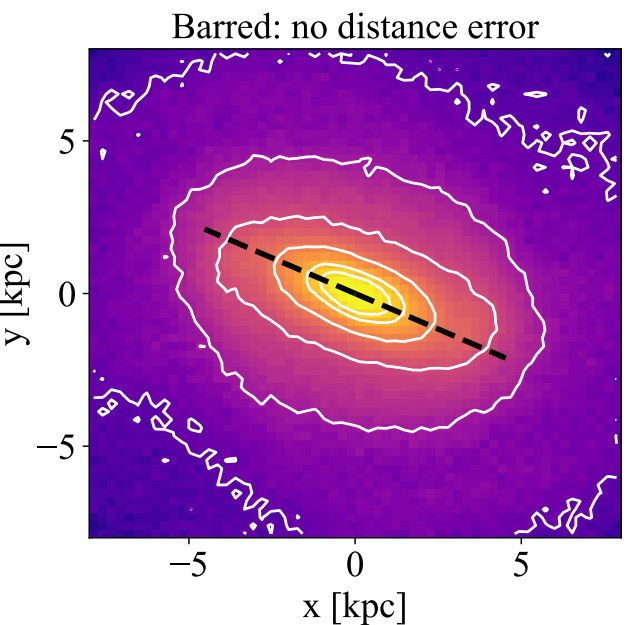
Before the spin-up



Quantify bar-driven dipole signature in $\Delta\nu_l$ map

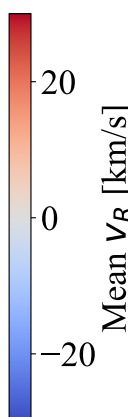
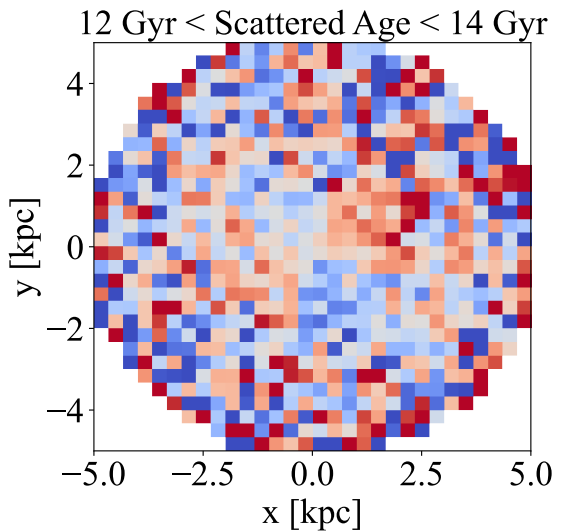
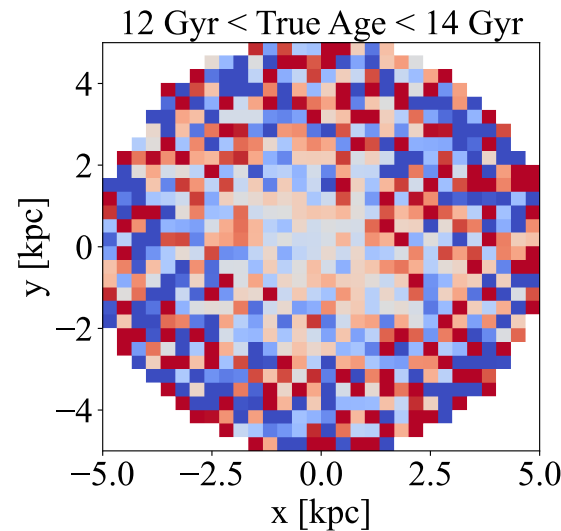
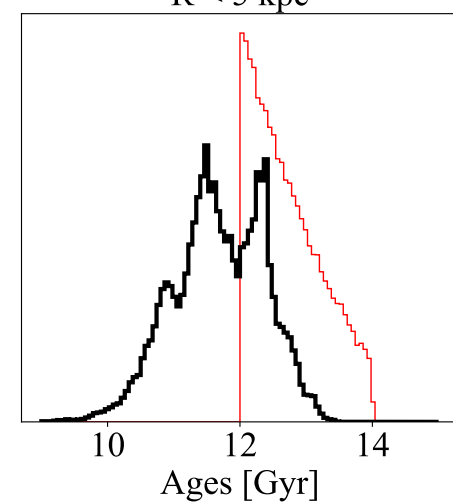
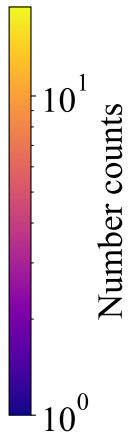
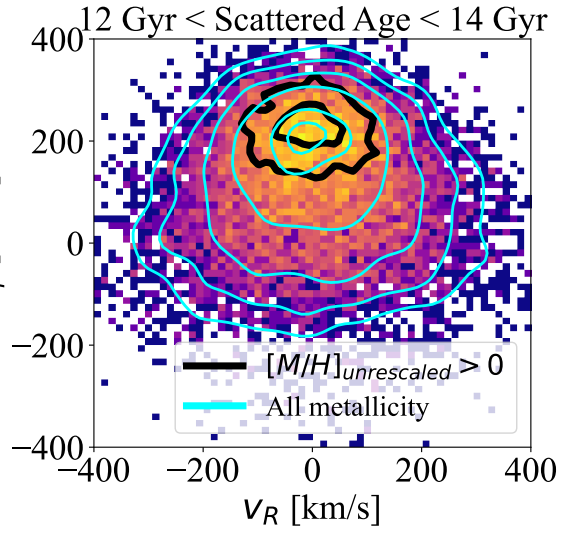
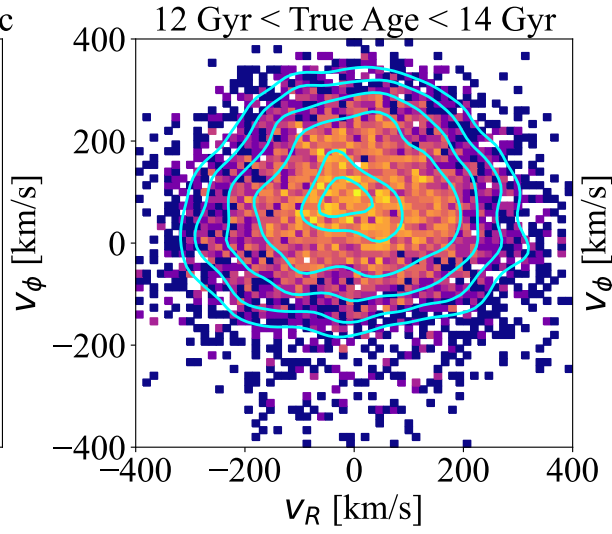
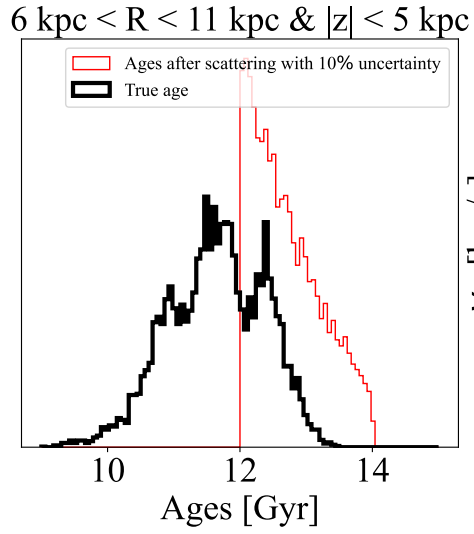


Effect of the distance uncertainty



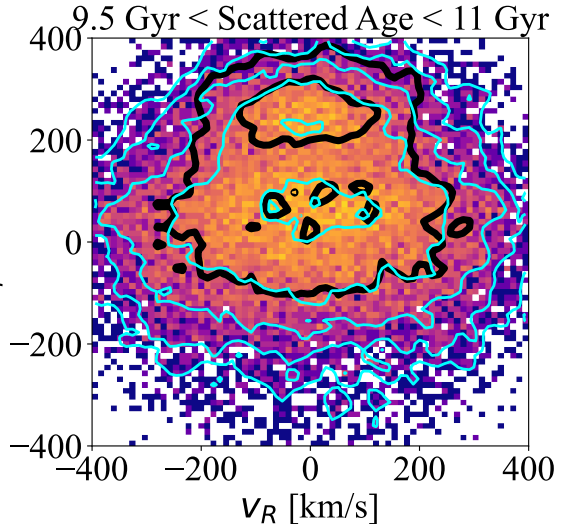
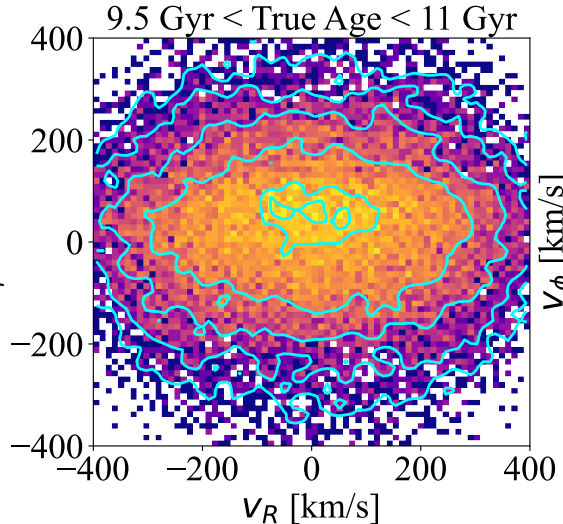
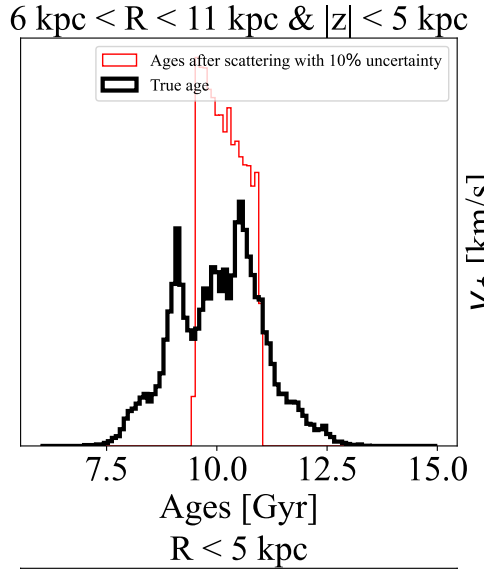
Effect of age uncertainty

Au18



Effect of age uncertainty

Au26



Number count

10^0

10^1

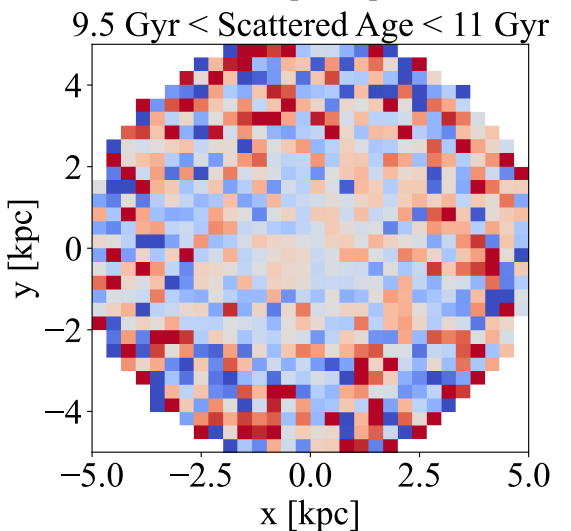
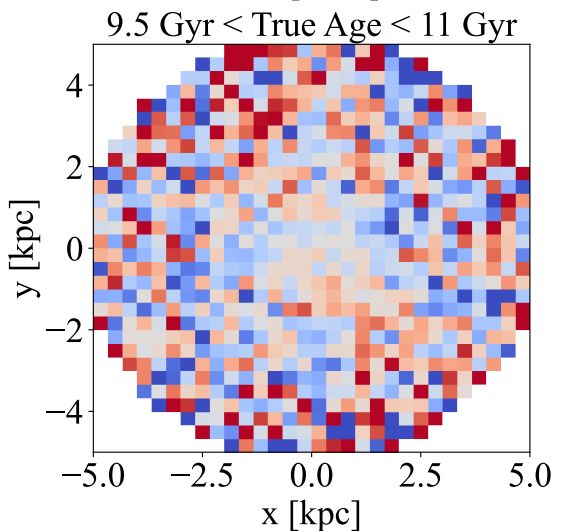
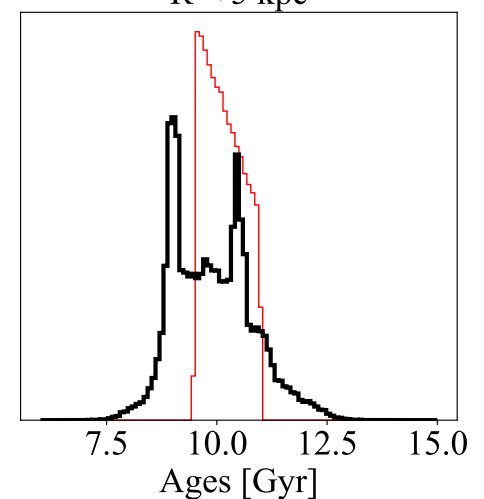
Mean v_R [km/s]

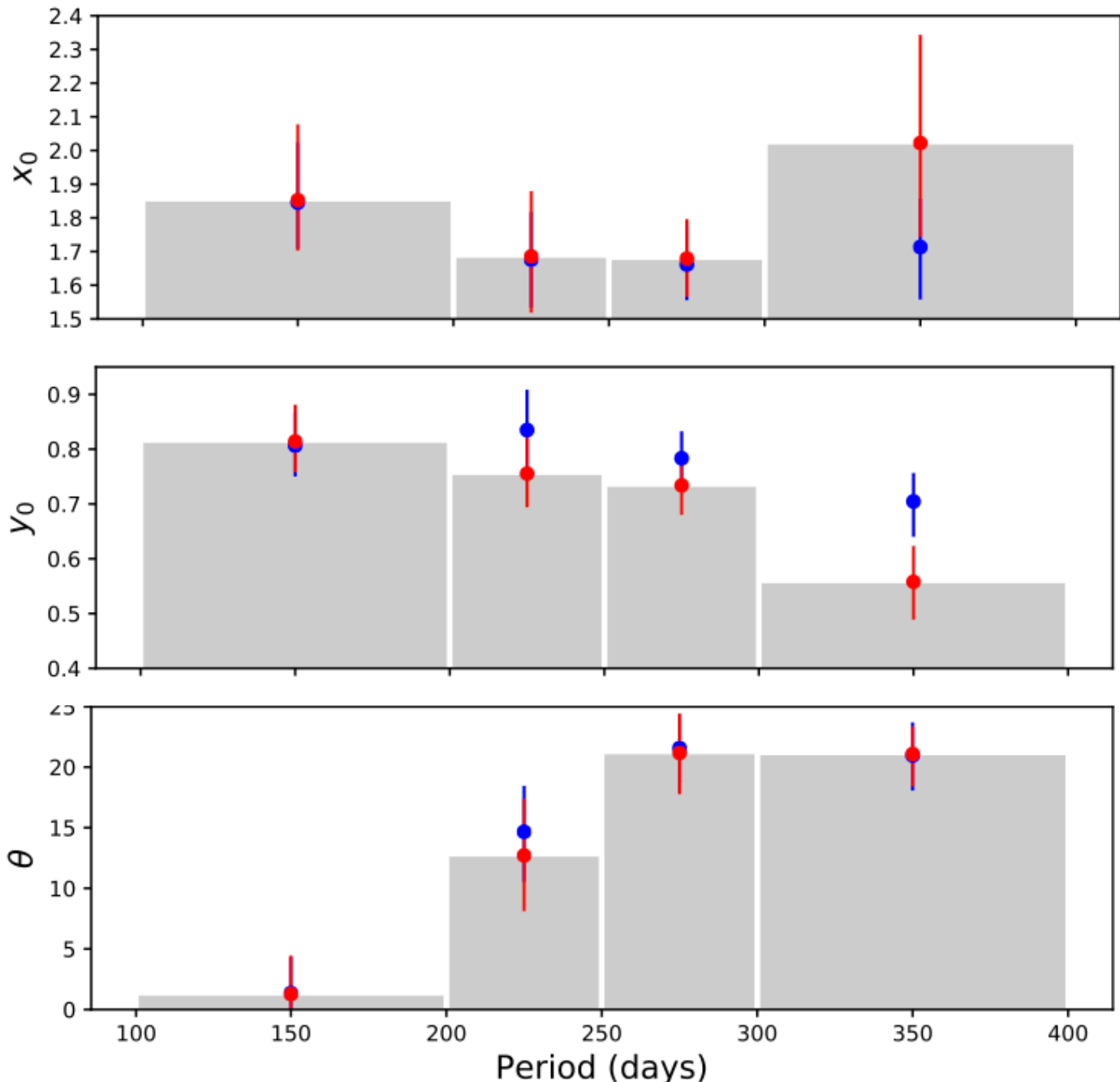
-20

0

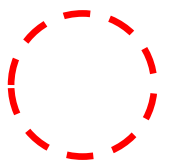
20

This figure contains two vertical color bars. The left one is labeled "Number count" and has logarithmic ticks at 10^0 and 10^1 . The right one is labeled "Mean v_R [km/s]" and has linear ticks at -20, 0, and 20.





Grady+ 2020



1 kpc spherical
spatial volume

- Stars in sample A
- ★ Stars in sample B

